Marine Micropaleontology 190 (2024) 102388

Contents lists available at ScienceDirect

Marine Micropaleontology

journal homepage: www.elsevier.com/locate/marmicro

Research paper

Unraveling ecological signals related to the MECO onset through planktic and benthic foraminiferal records along a mixed carbonate-siliciclastic shallow-water succession

Antonella Gandolfi [a,*], Victor Manuel Giraldo-Gómez [a], Valeria Luciani [b], Michele Piazza [a], Valentina Brombin [b], Simone Crobu [a], Cesare Andrea Papazzoni [c], Johannes Pignatti [d], Antonino Briguglio [a]

[a] Dipartimento di Scienze della Terra, dell'Ambiente e della Vita, Università di Genova, Corso Europa 26, 16132 Genova, Italy
[b] Dipartimento di Fisica e Scienze della Terra, Università di Ferrara, Via Giuseppe Saragat 1, 44100 Ferrara, Italy
[c] Dipartimento di Scienze Chimiche e Geologiche, Università di Modena e Reggio Emilia, Via Campi 103, I-41125 Modena, Italy
[d] Dipartimento di Scienze della Terra, Università degli Studi di Roma "La Sapienza", Piazzale Aldo Moro 5, I-00185 Roma, Italy

ARTICLE INFO

Keywords:
MECO
Liguria
Foraminifera
Shallow water
Isotopic records
Paleoenvironmental reconstruction

ABSTRACT

The shallow-water Capo Mortola succession (Liguria, NW Italy) yields diverse assemblages of smaller benthic and planktic foraminifera, larger benthic foraminifera (LBF), and calcareous nannofossils. With the aim of improving the understanding of the Middle Eocene Climatic Optimum (MECO) impact on the shallow-water marine biotic communities due to global warming, we provide biostratigraphic and stable isotope data to achieve a reliable stratigraphic constraint of the MECO. The correlation of the stable isotope oxygen data with datasets of similar age from other regions suggests that only the onset of the MECO interval is recorded in the Capo Mortola section. Quantitative analyses of smaller benthic foraminiferal assemblages indicate that the shallow-water setting of Capo Mortola was not particularly affected by the onset of the MECO perturbance because no variation in nutrient supply or oxygen level were detected. A different scenario is recorded by the LBF genera *Operculina* and *Discocyclina*, which increased in abundance across the MECO onset, probably due to a rise in temperature and adapting to the increase in nutrient supply. In the upper water column, the variations in calcareous plankton communities appear to be controlled by both the MECO warming and a moderate increase in eutrophic conditions related to the enhanced hydrological cycle. Nutrients, mostly consumed in the upper water column, reached the seafloor in a limited amount, as benthic foraminifera record a meso-oligotrophic environment across the studied MECO interval.

1. Introduction

Past climatic events and their impact on the marine biosphere permit inferences on possible ecological responses to future global warming scenarios. The Eocene epoch was a crucial, climatically dynamic interval when the highest temperatures were reached during both the Paleocene-Eocene Thermal Maximum (PETM) and the Early Eocene Climatic Optimum (EECO). The peak temperatures were followed by a long-term cooling trend that lasted through the middle and late Eocene (Zachos et al., 2001; Katz et al., 2008; Zachos et al., 2008; Bijl et al., 2010; Westerhold et al., 2020). This cooling trend has been reported as a "doubthouse" climate, which is comprised between the "hot and warmhouse" (sensu Westerhold et al., 2020) conditions of the early Paleogene (with high temperatures, high pCO_2 levels, and no permanent polar ice sheets) and the "cool and icehouse" regime (sensu Westerhold et al., 2020), which follows the establishment of the Antarctic continental ice sheet during the Priabonian and the Eocene-Oligocene transition (~34 Ma; Miller et al., 1987; Zachos et al., 1996; Zachos et al., 2001; Coxall et al., 2005; Miller et al., 2005; Katz et al., 2008; Zachos et al., 2008; Lear et al., 2008; Cramer et al., 2009; Anagnostou et al., 2016; Barr et al., 2022). The term "doubthouse" refers to the evidence that the cooling trend was not straightforward but interrupted by transient episodes of warming (Tripati et al., 2005; Sexton et al., 2006; Edgar et al., 2007; Bohaty et al., 2009), the most prolonged and intense of

* Corresponding author.
E-mail address: antonella.gandolfi@edu.unige.it (A. Gandolfi).

https://doi.org/10.1016/j.marmicro.2024.102388
Received 6 March 2024; Received in revised form 11 July 2024; Accepted 15 July 2024
Available online 24 July 2024

which was the Middle Eocene Climatic Optimum (MECO; Bohaty and Zachos, 2003). During the MECO, the $\delta^{18}O$ values of marine carbonate sediments and of benthic foraminifera tests declined by roughly 1‰ in over ~400 kyr, which is usually interpreted as a 4–6 °C rise in global temperature, with a gradual onset and a brief temperature peak centered at ~40 Ma followed by a rapid return to pre-event conditions (Bohaty and Zachos, 2003; Jovane et al., 2007; Zachos et al., 2008; Bohaty et al., 2009; Edgar et al., 2010; Luciani et al., 2010; Spofforth et al., 2010; Savian et al., 2013; Boscolo Galazzo et al., 2014; D'Onofrio et al., 2021).

The MECO is one of the most mysterious global warming events of the Cenozoic due to a number of factors, such as its longer duration with respect to the Eocene hyperthermals and the lack of a globally coherent negative $\delta^{13}C$ excursion in marine carbonates (Sluijs et al., 2013). It has been suggested that the MECO warming was triggered by atmospheric CO_2 increases by paroxysmal continental arc volcanism (Sluijs et al., 2013; van der Boon et al., 2021), even though the correlation of these events is not well constrained. Furthermore, precise data on paleoenvironmental changes and specific resilience of the biosphere across the MECO are still limited and are mostly focused on deep-water environments (Luciani et al., 2010; Edgar et al., 2013; Boscolo Galazzo et al., 2013, 2014; D'Onofrio et al., 2021).

Conversely, the impact of the MECO on biota in shallow-water settings is yet poorly investigated (Brachert et al., 2023; Gandolfi et al., 2023) despite the fact that shallow-water sedimentary records represent crucial archives to unravel how biodiversity reacted to global warming events. Shallow-water sedimentary successions are indeed more challenging to study in relation to climatic perturbations for several reasons, including the limited biostratigraphic resolution and the problems in correlation with deep-sea settings (Pekar et al., 2005). In addition to the global controls, shallow-water deposits are more influenced than deep-sea sediments by local tectonic patterns of sediment accretion and higher hydrodynamic activity that may induce unconformities. The MECO event was studied in a shallow-water setting (Sealza section), located in the Liguria region of northwestern Italy (Gandolfi et al., 2023). This section provides data from several taxonomic groups including smaller, larger benthic (SBF and LBF, respectively) and planktic foraminifera (PF), together with nannofossil and stable isotope data. The MECO interval in Sealza is characterized by a decrease in oxygenation at the seafloor, as indicated by a decline in the abundance of epifaunal taxa, an increase in organic matter content (TOC), and the occurrence of infaunal genera (Gandolfi et al., 2023).

The available literature on the MECO warming is almost only related to deep-sea successions and documents marked variations in planktic foraminiferal communities, such as a permanent decline in abundance of the large-sized mixed-layer dweller *Acarinina,* that has not yet been clearly explained, as this genus is recognized as warm index and thus should have benefited from the MECO warming (Luciani et al., 2010; D'Onofrio et al., 2021). The hypothesis that the loss of the symbiotic relationship with microalgae, adapted to thrive in oligotrophic environments, may have been responsible for the recorded decline was disproved by the record of a single transitory episode of bleaching (Edgar et al., 2013).

In shallow-water settings, the relationships between the foraminiferal assemblages and the MECO event are not fully understood either. Rodelli et al. (2018) gave some information regarding the LBF assemblages from the Baskil section (eastern Turkey), including high-resolution biostratigraphy and correlation with magnetostratigraphy, planktic foraminiferal, and calcareous nannofossil biozones; this section includes the MECO interval, but unfortunately the authors do not provide isotopic data and do not discuss the changes in LBF assemblages around this interval. Kövecsi et al. (2022), describing the nummulite banks from the Transylvanian Basin (Romania), pointed out that these peculiar accumulations are dated just above the inferred position of the MECO, thus implying that post-MECO conditions were suitable for the bloom of large species of the genus *Nummulites*. Morabito et al. (2024) reported a comprehensive study of the Monte Saraceno section (southern Italy), including LBF assemblages, high-resolution biostratigraphy, and isotopic data allowing to connect the nummulite accumulations with the MECO and post-MECO intervals, followed by the fading of very large nummulites up to the end of SBZ 17. According to these data, one may infer that the rise in temperatures had apparently a positive effect on the large nummulites, possibly followed by a gradual deterioration in the post-MECO, as evidenced by the faunal changes passing into the subsequent SBZ 18.

With the aim of improving the understanding of the MECO impact on the shallow-water marine communities as related to global warming, we present here the analysis of the Capo Mortola succession outcropping in Liguria (NW Italy; Fig. 1A). This section contains a diverse assemblage of both benthic and planktic foraminifera, as well as calcareous nannofossils, thus allowing an integrated approach. We provide biostratigraphic and stable isotope data to achieve a reliable stratigraphic constraint for the MECO. Quantitative analyses of the recorded taxa are also presented to highlight changes in fossil communities, which are essential to correctly evaluate the biotic response.

2. Geological setting

The promontory of Capo Mortola is located within the municipality of Ventimiglia and flanks the Hanbury Botanical Gardens (Fig. 1A, B1, B2, B3). The promontory itself and its prospicient submarine areas are included in the Hanbury Botanical Gardens Regional Protected Area, and rock sampling is forbidden without valid permission. Although the previous work by Carbone et al. (1981) provided a comprehensive sampling of the entire stratigraphic succession, this study focuses only on the upper part of the section (Fig. 1A, B1–B3, C).

From a lithostratigraphic perspective, the regional succession starts with the marly limestones of the Trucco Formation (Santonian-lower Maastrichtian), continues with the sporadic Microcodium Formation (which has very uncertain dating), and passes into the Capo Mortola Calcarenite (upper Lutetian-lower Bartonian according to the regional literature), which represents the first member of the Boussac/Sinclair Trilogy (Varrone and Clari, 2003; Sztrákos and du Fornel, 2003). The succession continues with the Olivetta San Michele Silty Marl (Marne a Globigerine = Globigerina marls: Bartonian-lower Priabonian) and ends with the Ventimiglia Flysch (upper Bartonian-lower Priabonian) (Gèze et al., 1968; Lanteaume, 1968; Carbone et al., 1981; Dallagiovanna et al., 2012; Seno et al., 2012; Coletti et al., 2021). The tectonic structure of this sector of the Provençal domain is mainly due to the superposition of the Alpine events on the Pyrenean-Provençal ones; the ensuing tectonic setting is subsequently involved in the Miocene deformations related to the Corsica-Sardinia Block anticlockwise rotation and in the Pliocene to Recent neotectonic events (Gèze et al., 1968; Lanteaume, 1968; de Graciansky et al., 2010; Giammarino et al., 2010; Dallagiovanna et al., 2012; Seno et al., 2012; Morelli et al., 2022).

The Capo Mortola Calcarenite Formation was deposited in the southeastern Provençal paleogeographic domain (Arc de la Roya, Southern Subalpine Chain, European Plate) (Giammarino et al., 2010; Seno et al., 2012), which comprises sedimentary rocks deposited from the Upper Cretaceous to the upper Eocene. During the Eocene, the Western and Ligurian Alps' orogenic wedge was thrust onto this region of the European Plate, resulting in the formation of a foreland-foredeep system (Lanteaume, 1968; Varrone, 2004; de Graciansky et al., 2010; Giammarino et al., 2010; Seno et al., 2012; Marini et al., 2022). The tectonically controlled sedimentation is characterized by shallow-water limestones grading upward to marlstones capped by siliciclastic turbidite deposits, known as the Priabonian Trilogy (Boussac, 1912) or Sinclair Trilogy (Sinclair, 1997).

The Capo Mortola section was measured along the western limb of the narrow, non-cylindrical syncline of Capo Mortola and exhibits a good exposure of the transgressive facies of the Capo Mortola Calcarenite Formation (known in the literature as Nummulitic Limestone = Calcareniti di Capo Mortola, Dallagiovanna et al., 2012; Seno et al.,

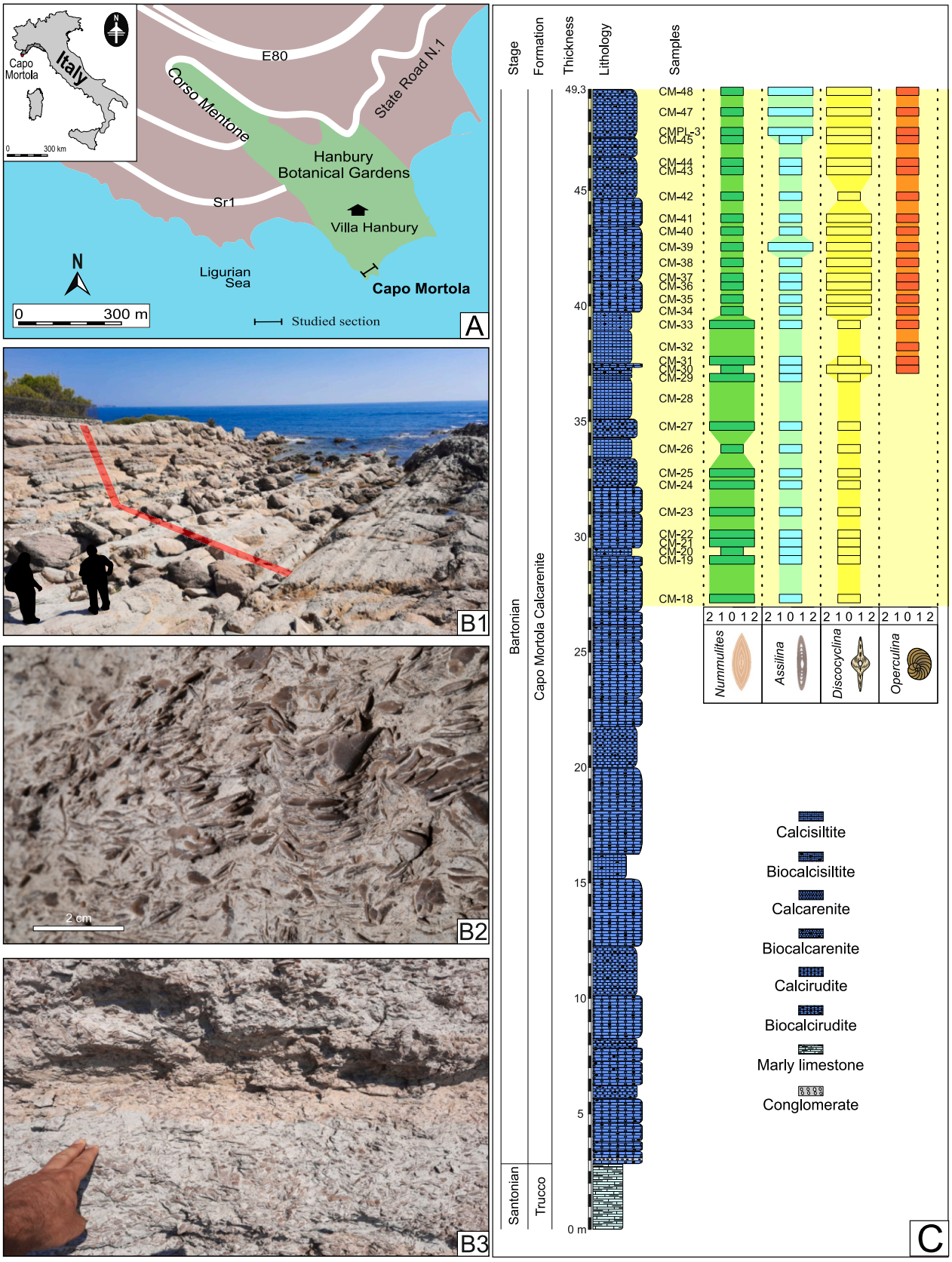

Fig. 1. A) Map showing the location of the Capo Mortola promontory (Liguria, NW Italy) and the studied section. B1) Outcrop in the upper part of the Capo Mortola section (red band); B2) LBF lining the wall of *Nummipera* burrows (near CM-38). B3) Outcrop photograph showing abundant tests of *Assilina* (about 1 cm in diameter) (near CM-31). C) Stratigraphic column of the Capo Mortola section (yellow shaded band represents the studied part) and relative abundances of LBF recorded in thin sections (0: absent; 1: common; 2: abundant). (For interpretation of the references to colour in this figure legend, the reader is referred to the web version of this article.)

2012) resting on the weathered marly limestones of the Trucco Formation. The Olivetta San Michele Silty Marl is very poorly exposed, and the Microcodium Formation does not crop out in the area.

3. Material and methods

3.1. Field sampling

The Capo Mortola section, from the base of the Capo Mortola Calcarenite Formation to the top of the exposition, has a total thickness of 49.3 m. The entire succession is shown in Fig. 1B1, C, and the lithological and paleontological description of all samples is reported as supplementary data. In this study, we focused on the interval from 27.0 to 49.3 m (Fig. 1B1, C), which records the major climatic perturbations that happened during the Bartonian.

The dataset comprises 30 rock samples that have been treated for foraminiferal analyses and 43 additional powder samples, obtained at around 30 cm intervals by pressure drillers (from 36.9 to 49.3 m; Figs. 1C, 2), used to extract carbon and oxygen stable isotopes. Due to intense local weathering and sea wave action on the rock surfaces, powder samples were collected after drilling an initial hole at least 2 cm deep. The powder was collected using a funnel and then immediately placed in polypropylene vials for storage.

3.2. Stable isotopes

The carbon and oxygen stable isotope analyses were performed at the Laboratory of Paleoclimatology and Isotopic Stratigraphy of the Department of Physics and Earth Sciences of the University of Ferrara, using isoFLOW (Elementar©) operating in continuous flow with a PrecisION Isotopic Ratio Mass Spectrometer (IRMS; Elementar©). The 43 powder samples (CMP1-CMP43) were tested; roughly 150 g of homogeneous powder was weighted and placed in vials. To replace the ambient air in the glass tube, each vial was flushed with pure He using a needle situated in the autosampler. The powder in each vial reacted with heated, viscous, water-free orthophosphoric acid for 3 h at 50 °C, causing CO_2 to be released from the samples. The released CO_2 sample gas was collected and transported to the IRMS for simultaneous C and O analysis using the same needle that had previously flushed the vial. The $^{13}C/^{12}C$ and $^{18}O/^{16}O$ isotopic ratios were expressed with the δ notation (in ‰ units) relative to V-PDB. The in-house MAQ-1 standard was used for single-point calibration, and the quality of the analysis was monitored using two control standards (IAEA 603 and Carrara Marble). The analytical uncertainties (1 σ) for the isotope studies were in the range of

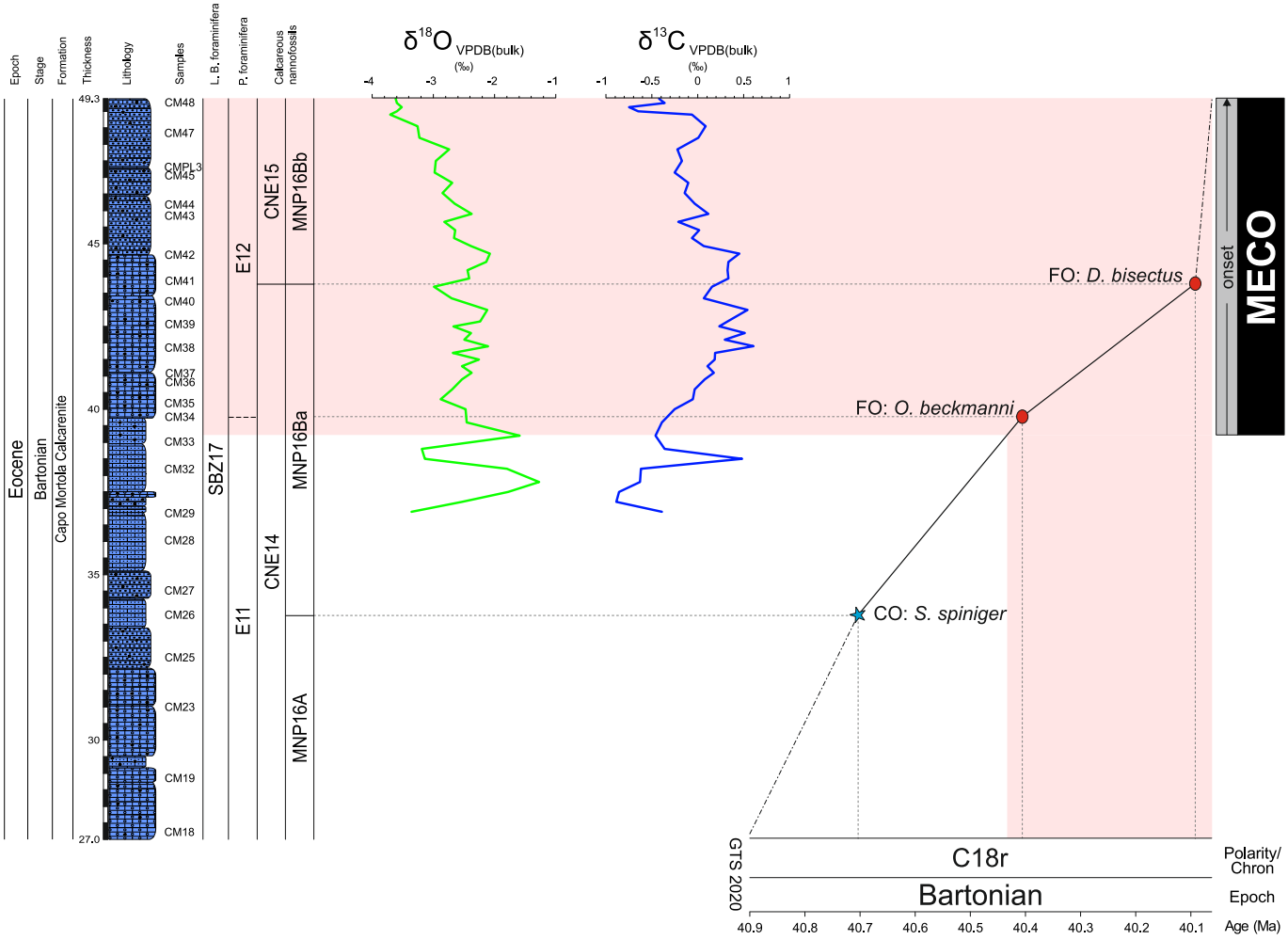

Fig. 2. Oxygen ($\delta^{18}O$, green line) and Carbon ($\delta^{13}C$, blue line) isotope data from bulk samples plotted against the stratigraphic log of the Capo Mortola section and LBF biozones (SBZ following Serra-Kiel et al., 1998), planktic foraminifera (E zones following Wade et al., 2011), and calcareous nannofossils (MNP zones following Fornaciari et al., 2010 and CNE zones following Agnini et al., 2014). Biostratigraphy and age model of the Capo Mortola section for the middle Eocene based on calcareous nannofossil and planktic foraminifera events. The composite standard reference section (CSRS) of the middle Eocene (Bartonian) shows the absolute age model of Speijer et al. (2020). The pink-shaded band outlines the Middle Eocene Climatic Optimum (MECO) onset correlated to Chron C18r, according to Speijer et al. (2020). (For interpretation of the references to colour in this figure legend, the reader is referred to the web version of this article.)

±0.1 ‰ for $\delta^{13}C$ and $\delta^{18}O$, respectively.

3.3. Foraminifera

Planktic and smaller benthic foraminifera were successfully extracted from rock samples using the surfactant Rewoquat© W 3690. The procedure consists of crushing samples into pieces of size 1–2 cm using a mechanic press and then soaking them in pure Rewoquat© for two days. Each sample was then washed through a single 63 μm-mesh sieve, and the residues were dried at 50 °C. Microfossils were picked, placed in microslides, and identified under a binocular stereomicroscope (Optech GZ808) equipped with an Invenio 6EIII DeltaPix camera. The taxonomic criteria adopted in this study are based on Loeblich and Tappan (1987, 1994) and Holbourn et al. (2013) for benthic foraminiferal genera, whereas Pearson et al. (2006) was used for planktic foraminiferal taxa. Washed residues were split (microsplitter) to a workable amount to get, whenever possible, at least 300 specimens per sample, and then standardized to 2 g of dried sediment and expressed as a percentage (see Supplementary data). Benthic and planktic foraminiferal absolute abundances, retrieved from the picking procedure, are abbreviated as BFN and PFN, respectively. In addition, the ratio between planktic and benthic foraminifera was evaluated as P/(P + B) *100 as a tool to establish the paleodepth (van der Zwaan et al., 1990).

Larger benthic foraminifera (LBF), mostly too large to be retrieved in the washed material (except for the genus *Operculina*), were studied from rock-thin sections. Equatorial sections were obtained by grinding specimens directly collected on the outcrop surface; in the case of hard lithology, rock samples were soaked in a Rewoquat© for ~two days to isolate the LBF tests. A total of 274 oriented sections have been prepared and analyzed, and most of them permit identification at species level. Whenever possible and reliable, subspecies identification was achieved, mostly on discocyclinids. To identify the nummulitids, we adopted the typological criteria by Herb and Hekel (1975) and Schaub (1981), which require a variety of biometric measurements. The taxonomic criteria for discocyclinids, followed by Özcan et al. (2006, 2022), also required numerous biometric data measurable on each equatorial section.

For LBFs, this study adopted the biozonation SBZ (Shallow Benthic Zones) of Serra-Kiel et al. (1998) as amended by Papazzoni et al. (2017), while the zonal scheme of Orthophragminid Zones (OZ) by Özcan et al. (2022) was adopted for the discocyclinids. Planktic foraminiferal biozones were identified,according to Wade et al. (2011).

3.4. Calcareous nannofossils

Fourteen samples from the Capo Mortola section, covering the interval from 27.0 to 49.3 m, were analyzed as smear-slides using the standard techniques of preparation (see Bown and Young, 1998). Semi-quantitative biostratigraphic analysis was performed using transmitted-light microscopy (Leitz) in cross-polarized (XPL) and phase contrast (PC) light at ~1000× magnification. Semi-quantitative data were recorded by scanning five traverses of each slide (see Supplementary data). For this reason, five abundance classes are recorded following Gandolfi et al. (2023): very abundant (D: taxon with abundances >50% of the assemblage), abundant (A: 5 specimens per field of view (FOV), common (C: 1–5 specimens per FOV), few (F: 1 specimen per 1–10 FOV), and rare (R: 1 specimen per >10 FOV). Calcareous nannofossils were identified to species level where possible following the taxonomy of Perch-Nielsen (1985) and Nannotax (Young et al., 2022). This study adopted the biozonations MNP and CNE by Fornaciari et al. (2010) and Agnini et al. (2014), respectively.

4. Results

4.1. Biostratigraphy

In this study, biostratigraphy relies on planktic foraminifera, calcareous nannofossils, and larger benthic foraminifera; all biozones identified are shown in Fig. 2. In terms of planktic foraminifera, we were able to identify the Total Range Zone E12 (Wade et al., 2011), which largely corresponds to the MECO interval (Sexton et al., 2006; Bohaty et al., 2009; Agnini et al., 2021), as evidenced by the occurrence of *Orbulinoides beckmanni* in the interval from 39.7 to 49.2 m. The interval below the base of *O. beckmanni* is referred to as Zone E11 due to the absence of *Guembelitrioides nuttallii* and *O. beckmanni*.

Calcareous nannofossils in the Capo Mortola section vary between poorly and well preserved; they are generally scarce in almost all calcirudites and calcarenites but more abundant in samples that correspond to fine-grained calcisiltite. In all studied samples,reworked Cretaceous taxa occurred, but this did not hamper the biostratigraphic attribution of the Eocene succession. The most significant species recognized are illustrated in Fig. 3. According to the biozonation study by Agnini et al. (2014), we identified two biozones. Biozone CNE14 (27.3 m - 43.7 m) is characterized by the common occurrence (CO) of *Reticulofenestra reticulata*, *R. umbilicus*, and *Sphenolithus furcatolithoides*. This biozone spans an interval of 16.4 m between samples CM-18 and CM-38. Biozone CNE15 (43.7–49.3 m) is marked by the first occurrence (FO) of *Dictyococcites bisectus* in sample CM-41 (43.7 m), and this zone continues until the top of the studied section.

Likewise, three biozones are recognized according to the biozonation by Fornaciari et al. (2010). Biozone MNP16A (27.3–33.7 m) is indicated by the common presence of *S. furcatolithoides* and the occurrence of *R. reticulata* and *R. umbilicus*. In sample CM-26, *S. furcatolithoides* is more abundant than the previous one. Successively, the biozone MNP16Ba (33.7–43.7 m) is defined by the continuous occurrence of *Sphenolithus spiniger* between the high occurrence (HO) of *S. furcatolithoides* and the lowest common occurrence (LCO) of *D. bisectus*. This biozone is characterized by the common presence of *Dictyococcites scrippsae*, *R. reticulata*, *Coccolithus pelagicus*, and *Cyclicargolithus floridanus*. Finally, the biozone MNP16Bb (43.7–49.3 m) is determined by the FO of *D. bisectus* and the common and continuous occurrence of *S. spiniger*. This biozone correlates with biozone CNE15 and continues until the top of the studied section. Within this zone, it is possible to record the common presence of *D. scrippsae*, *R. reticulata*, *C. pelagicus*, *C. floridanus*, and *S. spiniger*.

Larger benthic foraminifera are represented by species indicating SBZ 17. The assemblage is dominated by *Nummulites perforatus*, *N. biarritzensis*, *N. puigsecensis*, and *N. striatus* (Fig. 4). Among these species, *N. puigsecensis* is considered by Serra-Kiel et al. (1998) as limited to SBZ 16; however, the range of this species is reported as extended to the Bartonian ("Biarritzian") by both Schaub (1981) and Serra-Kiel (1984). Therefore, we consider the range of *N. puigsecensis* as SBZ 16–17. As regards *N. striatus*, reported as SBZ 18–19 (lower part) by Serra-Kiel et al. (1998), we follow Seddighi et al. (2015), extending its stratigraphic range also to SBZ 17.

The only species recovered belonging to the genus *Assilina* is *A. exponens*. The most common orthophragminids are *Discocyclina pulchra baconica* and *D. dispansa sella*. Toward the uppermost part of the profile, two more subspecies occur: *D. augustae olianae* and *D. trabayensis elagizensis*, which are all related to OZ 13 and could start from sample CM-45. This indicates that the succession was deposited during the uppermost part of SBZ 17, possibly very close to the boundary with SBZ 18.

4.2. Trends in oxygen and carbon stable isotope values

The results of bulk oxygen and carbon stable isotope analyses are shown in Fig. 2; the $\delta^{18}O_{VPDB(bulk)}$ values vary between −3.7‰ and

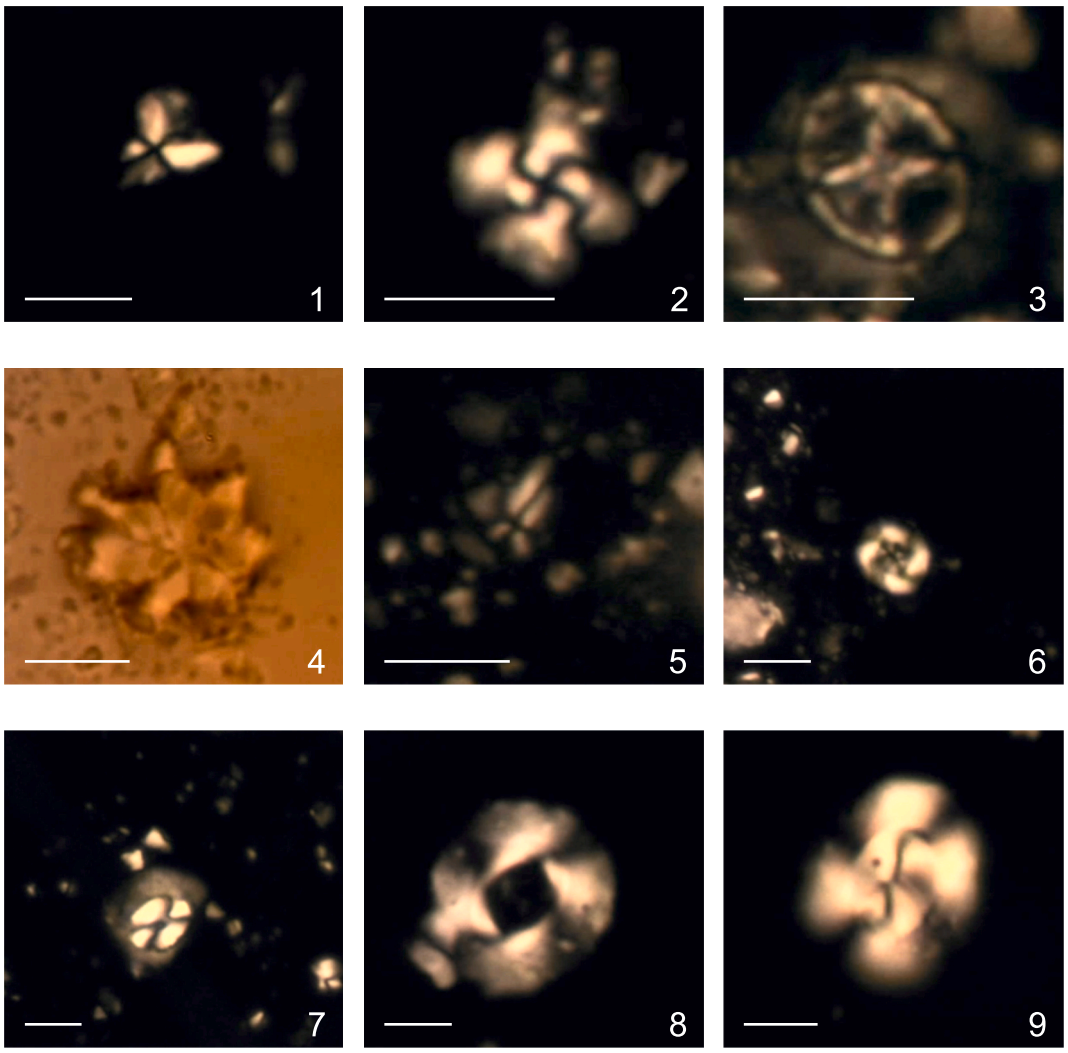

Fig. 3. Photomicrographs of selected calcareous nannofossils from the Capo Mortola section. The scale bar of 5 μm applies to all figs. 1. *Sphenolithus spiniger* Bukry, 1971 (CM-26); 2. *Dictyococcites scrippsae* Bukry and Percival, 1971 (CM-42); 3. *Chiasmolithus* sp. (CM-45); 4. *Discoaster* sp. (CM-32); 5. *Sphenolithus furcatolithoides* Locker, 1967 (CM-26); 6. *Reticulofenestra reticulata* (Gartner and Smith, 1967) Roth and Thierstein, 1972 (CM-33); 7. *Coccolithus pelagicus* (Wallich, 1877) Schiller, 1930 (CM-41); 8. *Reticulofenestra umbilicus* (Levin, 1965) Martini and Ritzkowski, 1968 (CM-33); 9. *Dictyococcites bisectus* (Hay, Mohler and Wade 1966) Bukry and Percival, 1971 (CM-42).

−1.2‰ with two positive peaks at 37.8 and 39.2 m and two negative peaks at 38.5 and 38.8 m. Several minor shifts toward higher or lower values are recorded between −3‰ and −2‰, but with an increasingly negative overall trend ending at −3.7‰.

The $\delta^{13}C_{VPDB(bulk)}$ values vary between −0.8‰ and 0.6‰, with one positive peak at 38.5 m. The $\delta^{13}C_{bulk}$ curve records show a slight increase from 37.2 to 43.0 m with several major/minor shifts and values around 0‰ and 0.5‰, followed by a decrease from 49.0 m with values moving between −0.5‰ and 0‰. In addition, there are two negative peaks at 49.0 and 49.1 m with values of −0.6‰ and −0.7‰, respectively, followed by a return to values between −0.5‰ and 0‰.

In the Capo Mortola section, variations in isotopic values linked to lithostratigraphic changes, as seen in the Sealza section (Gandolfi et al., 2023), are not observable.

4.3. Foraminiferal abundances

The preservation of both benthic and planktic foraminiferal tests is sufficient to correctly identify the genera and sometimes the species. The abundances of benthic and planktic foraminifera are shown in Figs. 5 and 6, respectively, and the most significant taxa are illustrated in Fig. 7.

From the disaggregated samples, a total of eight smaller and one larger benthic foraminiferal genera were recognized (Fig. 5). With the only exception of *Operculina*, which was found in washed residues, larger foraminifera such as *Nummulites*, *Assilina*, and *Discocyclina* have not been retrieved in the disaggregated samples and are treated separately in thin sections (Fig. 1C). The most abundant genus is *Heterolepa* (*H. dutemplei;* mean abundance 40.4%), which is characterized by some oscillations from 27.3 to 39.0 m and displays a slight abundance decrease from 39.0 to 41.0 m, followed by a return to the previous abundance that remains constant in the upper part of the section. The genus *Cibicidoides* (mean abundance 12.5%) shows its maximum abundance in the lower part of the selected interval, followed by a decrease from 31.0 to 38.3 m and then a further increase at 39.0 m. A similar trend is followed by the genus *Anomalinoides*, sparsely occurring in the lower part of the selected interval. The genus *Operculina* (mean value: 12.2%) is almost absent from 27.3 to 39.0 m (occurring only in samples CM-23 and CM-28), but it markedly increases from 39.0 m to the end of the section. The infaunal genus *Uvigerina* is scarcely represented in this section (mean value: 1.5%), especially from 39.0 to 49.3 m. The major peaks of abundance occur at 33.7, 36.0, and 39.7 m. Other minor increases are recorded in the upper part of the section. The genera *Nodosaria* and *Quinqueloculina* occur only in samples CM-28, CM-32, CM-45, CMPL3, and CM-48, constituting a minor component of the

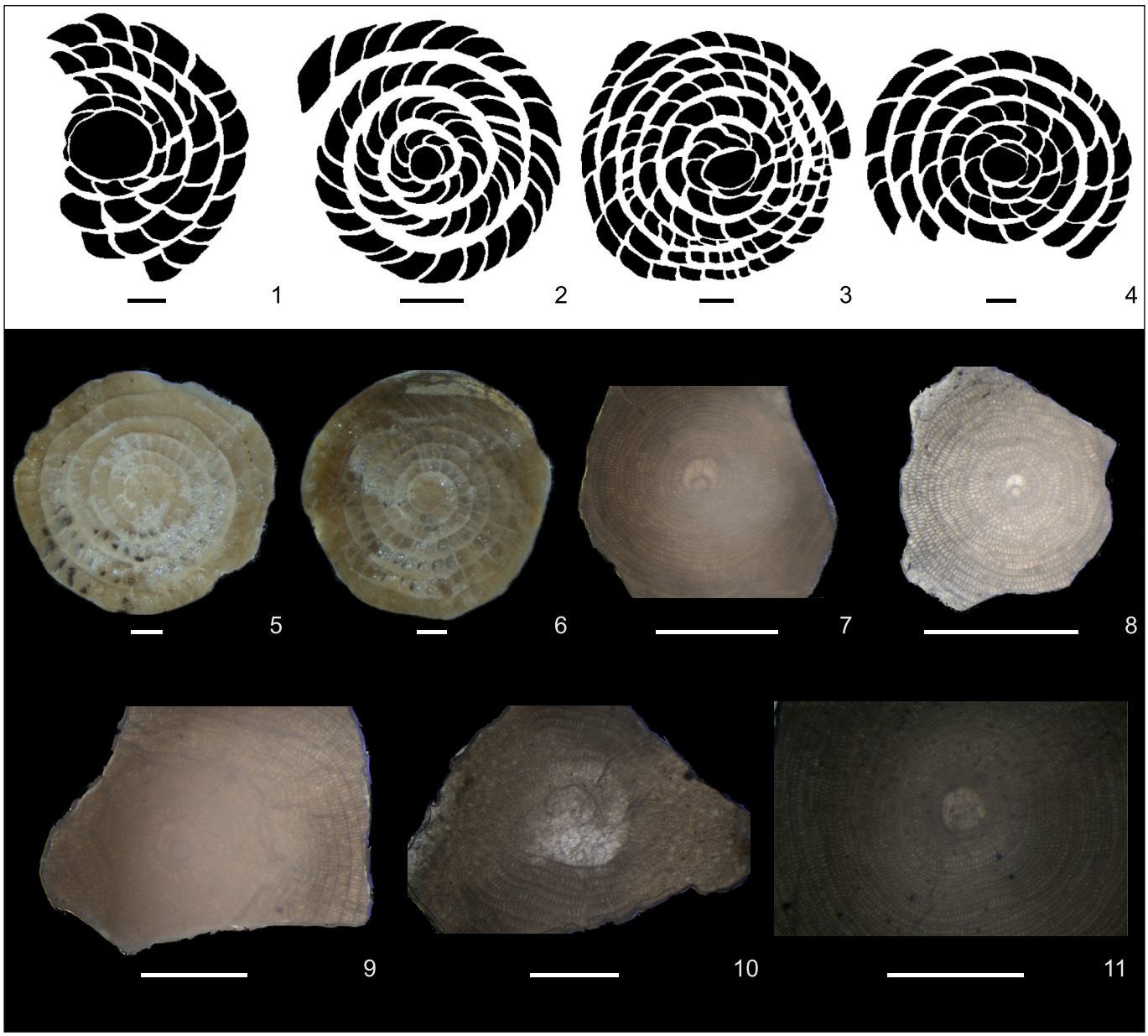

Fig. 4. Drawings and photomicrographs of selected larger benthic foraminifera from the Capo Mortola section. Scale bars of 1 mm apply to all figs. 1. *Nummulites puigsecensis* (CM-5); 2. *Nummulites incrassatus* (CM-5); 3. *Nummulites perforatus* (CM-8); 4. *Nummulites brongniarti* (CM-6); 5. *Assilina exponens* (CM-40); 6. *Assilina exponens* (CM-35); 7. *Discocyclina radians radians* (CM-40); 8. *Discocyclina augustae olianae* (CM-41); 9. *Discocyclina pratti pratti* (CM-38); 10. *Discocyclina pulchra baconica* (CM-39); 11. *Discocyclina dispansa sella* (CM-40).

assemblages. In turn, *Lenticulina* and *Dentalina* do not show significant changes in abundance and are present almost continuously from the base to the top of the interval analyzed. These last four genera mentioned, scarcely represented, are indicated in Fig. 5 as "other benthics."

As for planktic foraminifera, five taxa were identified: *Subbotina hagni, S. eocaena*, *Acarinina praetopilensis, Morozovelloides* sp., and *Orbulinoides beckmanni* (Fig. 6). The most abundant genus is *Subbotina* (mean value 17.3%), which is recorded in all samples and shows an increase in abundance from 32.5 to 38.3 m, followed by a decrease at 38.3 m. Above this decrease, the abundance of *Subbotina* gradually recovers up to the top section. The genus *Acarinina* is less abundant than *Subbotina* but follows a similar trend, with an increase in abundance in the interval from 32.5 to 38.3 m, with three peaks at 33.7, 36.0, and 38.3 m. The main difference with *Subbotina* is that *Acarinina* is very scarce, from 39.0 m to the top of the profile. The genus *Morozovelloides* is absent in the lower part of the section and occurs from 40.8 to 49.3 m, albeit with very low percentages and minor oscillations; it increases in abundance in the uppermost portion of the section. Finally, *Orbulinoides beckmanni* is recorded in the interval spanning from 39.7 to 49.3 m in each sample, except for CM-36, CM-39, and CM-41.

5. Discussion

5.1. Isotopic record of the MECO

The Capo Mortola section displays a marked negative excursion of ~1‰ of the $\delta^{18}O_{bulk}$ in the interval from 39.20 to 49.30 m. Nevertheless, this negative excursion is correlated with the E12 biozone as well as with CNE14 and 15, so it is here interpreted as chronologically related to the MECO event (Fig. 2; Bohaty and Zachos, 2003; Sexton et al., 2006; Edgar et al., 2007; Bohaty et al., 2009; Edgar et al., 2010; Boscolo Galazzo

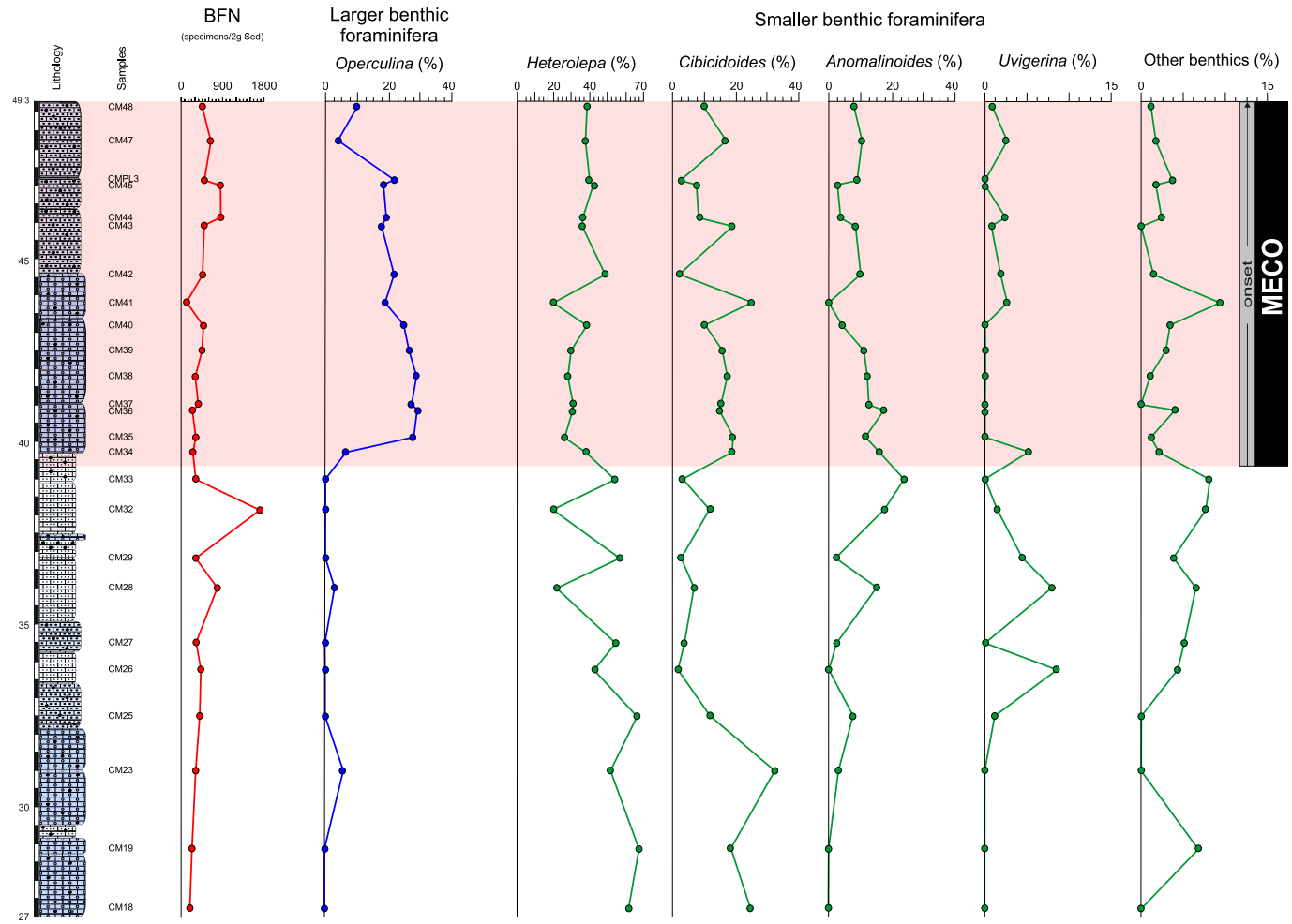

Fig. 5. Abundances of selected LBF and SBF foraminiferal genera (>63 μm fraction) before and across the onset of the MECO (pink-shaded band) in the Capo Mortola section plotted against lithology and samples collected. The genus *Discocyclina* is very abundant from meter 40 to 45. BFN: benthic foraminiferal number (specimens/2 g sediment); other benthics include the minor components of the assemblage (*Lenticulina*, *Nodosaria*, *Quinqueloculina*, and *Dentalina*). (For interpretation of the references to colour in this figure legend, the reader is referred to the web version of this article.)

et al., 2014; Borelli et al., 2014; Giorgioni et al., 2019). Correlating the $\delta^{18}O_{bulk}$ curve of the Capo Mortola section with those from other settings (Fig. 8), it is possible to interpret our data as limited only to the onset of the whole event. The composite standard reference section shown in Fig. 2 allows us to fix the onset recorded by the $\delta^{18}O_{bulk}$ signal at 40.43 Ma and its minimum peak at 40.06 Ma, thus resulting in approximately 370 kyr. The duration of this event (onset and peak) is estimated to be ~500 kyr, as recorded worldwide in deep-water settings (Bohaty and Zachos, 2003; Sexton et al., 2006; Bohaty et al., 2009; Edgar et al., 2010). Nonetheless, in some sections of the Neo-Tethys, the MECO is reported to have a longer duration of ~600 kyr (Bohaty et al., 2009; Edgar et al., 2010; Bijl et al., 2010; Witkowski et al., 2014; Giorgioni et al., 2019). This evidence is consistent with our assumption that only the onset of MECO is recorded at Capo Mortola.

The $\delta^{18}O_{bulk}$ record from the Capo Mortola section shows absolute values that are more negative than those obtained from the deep-water sites (Bohaty et al., 2009; Edgar et al., 2010; Spofforth et al., 2010). In turn, negative values of the $\delta^{18}O_{bulk}$ records have been linked to deltaic environments, which were coupled with diagenetic processes (Gandolfi et al., 2023; Peris-Cabré et al., 2023). Despite the differences in the $\delta^{18}O_{bulk}$ absolute values, the isotopic signal of the Capo Mortola section correlates clearly with similar data from other sections that register the incipient stage of the MECO onset, thus providing new perspectives into the MECO in mixed carbonate-siliciclastic shallow-water environments (Fig. 9). However, we cannot exclude that the lower $\delta^{18}O_{bulk}$ values recorded at Capo Mortola are also influenced by a diagenetic overprint on the primary isotopic signal or other alteration factors (Fig. 9) (Marshall, 1992; Schrag et al., 1995).

Diagenetic alteration has a more pronounced effect on oxygen isotopes than on carbon isotopes because of the high amount of oxygen relative to carbon present in post-depositional fluids (Marshall, 1992; Schrag et al., 1995; Fio et al., 2010). For this reason, carbonates with low $\delta^{18}O$ values can originate from freshwater input, increasing temperature, and meteoric diagenesis, whereas ^{18}O enrichment could suggest either a lower temperature or evaporation. On the contrary, carbon isotopes are more resistant to diagenetic alteration because they are not influenced by temperature (Marshall, 1992; Patterson and Walter, 1994; Schrag et al., 1995; Peris-Cabré et al., 2023). However, the values of $\delta^{13}C_{bulk}$ can be strongly modified by other factors such as the organic matter source, water circulation, extra-basinal carbonate input, stratification, runoff supply, and weathering (Saltzman and Thomas, 2012; Giraldo-Gómez et al., 2017; Läuchli et al., 2021; Peris-Cabré et al., 2023).

The degree of diagenetic alteration recorded in the Capo Mortola section is possibly attributed to post-depositional pore water carbonate disequilibria (low values of $\delta^{13}C_{bulk}$, $\delta^{18}O_{bulk}$; Fig. 9), due to partial organic matter oxidation. These lower values of $\delta^{18}O$ are probably linked to both burial diagenesis often recorded in proximal settings (e.g., Lavastre et al., 2011), and the subsequent tectonic deformation, well constrained in the region. Indeed, the thin sections observed from the

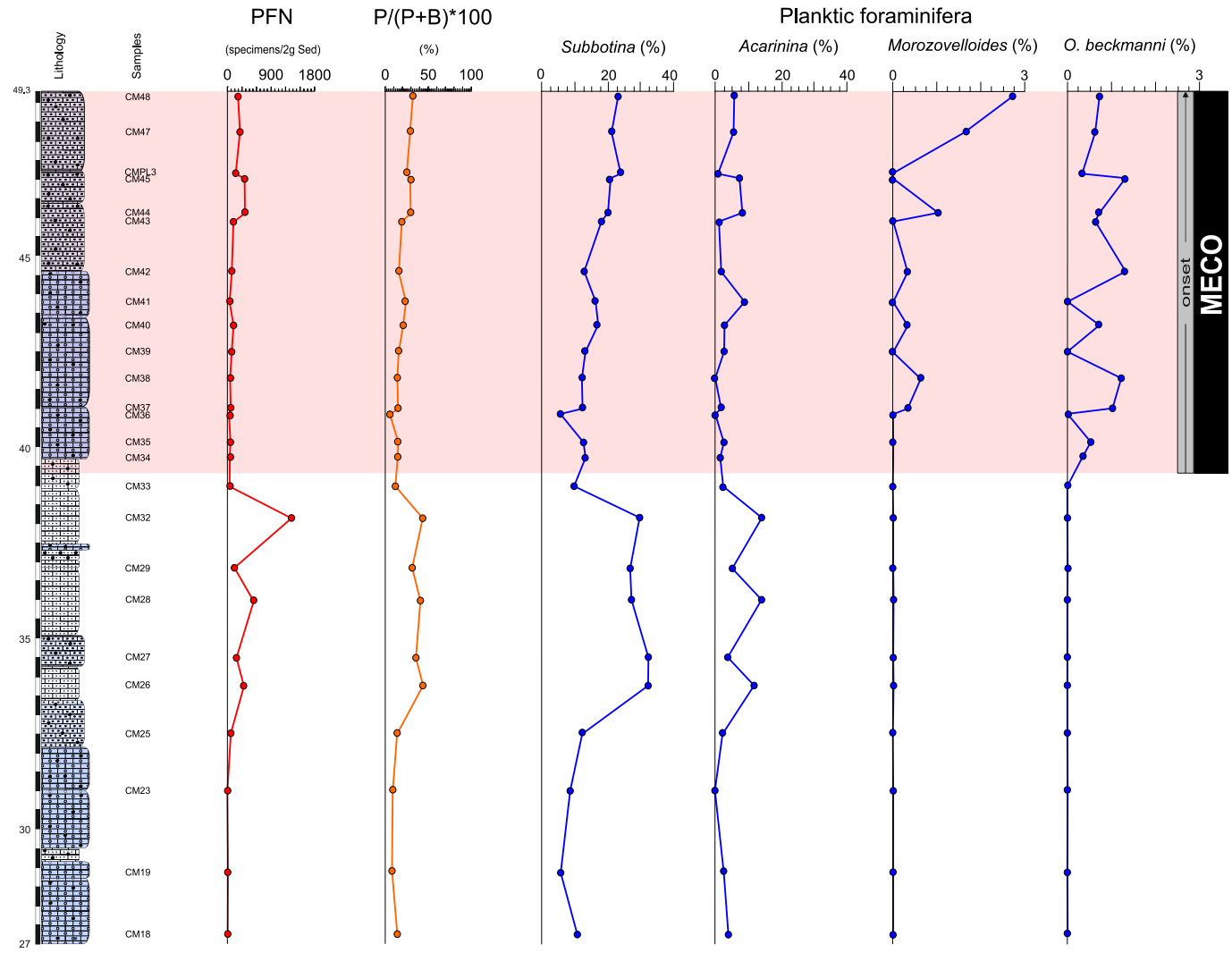

Fig. 6. Abundances of planktic foraminiferal genera (>63 μm fraction) before and during the MECO onset (pink-shaded band) in the Capo Mortola section plotted against lithology and samples collected. PFN: planktic foraminiferal number (specimens/2 g sediment); P/B: planktic to benthic (P/B) ratio calculated as P/(P + B) *100 and expressed as percentages of planktic foraminifera in the total foraminiferal assemblage. (For interpretation of the references to colour in this figure legend, the reader is referred to the web version of this article.)

Capo Mortola succession show intense fragmentation of nummulitic tests as evidence of burial and compaction, all further compromised by tectonic folding. Consequently, pore water chemistry differs from the original seawater chemistry, and the original isotopic signal could be altered (Veizer et al., 1999; Zachos et al., 2001; Giraldo-Gómez et al., 2017). These features can explain the lack of correlation between the $\delta^{13}C_{bulk}$ curve from Capo Mortola and the deep-sea records.

5.2. Environmental conditions at the seafloor

The investigation of the benthic foraminiferal assemblages from the Capo Mortola section, coupled with isotopic records, provides evidence of the paleoenvironmental changes across the MECO onset that differ from those known from the coeval Sealza section, cropping out a few kilometers northward (Gandolfi et al., 2023).

The great abundance of *Heterolepa*, together with common *Cibicidoides* (Fig. 5), during the pre-MECO interval suggests a well-oxygenated seafloor and poor nutrient supply because these genera are recognized as epifaunal benthic foraminifera living in well-oxygenated environments (van der Zwaan, 1982; Speijer, 1994; Speijer and Schmitz, 1998; Rögl and Spezzaferri, 2002; Giraldo-Gómez et al., 2018a, 2018b; Russo et al., 2022). In the MECO onset interval, although *Heterolepa* records a slight decrease in abundance, low nutrient supply to the seafloor and well-oxygenated conditions are confirmed by abundant LBF (Fig. 1) and the scarcity of infaunal taxa like *Uvigerina*. Interestingly, in this interval, the abundances of *Heterolepa* and *Cibicidoides* look out of phase, indicating probably a competition between these two genera for life resources and/or specific hydrodynamic preferences on the seafloor, given the fact that *Cibicidoides* might prefer more agitated waters than *Heterolepa* (Murray, 2006). Smaller benthic foraminifera however, were not particularly impacted by the onset of the MECO perturbance and therefore no significant variations either in nutrient supply or in oxygen level are interpreted. Conversely, in the shallow-water Sealza section (Gandolfi et al., 2023), in the lower part of the MECO interval, possibly correlating with the onset of the event at Capo Mortola, increased eutrophication and scarcely oxygenated seafloor conditions are clearly documented by modifications in benthic foraminiferal communities.

Additional clues are provided by abundance and distribution data of LBF (Fig. 1), which should normally thrive on illuminated seafloors and flourish in nutrient-depleted environments. Both *Operculina* and orthophragmines are abundant in the uppermost part of the section (Fig. 5), which suggests deposition in the deeper part of the photic zone, at depths below 50 m and below the storm weather wave base (Molina et al., 2016; Briguglio and Rögl, 2018; Kövecsi et al., 2022; Arena et al.,

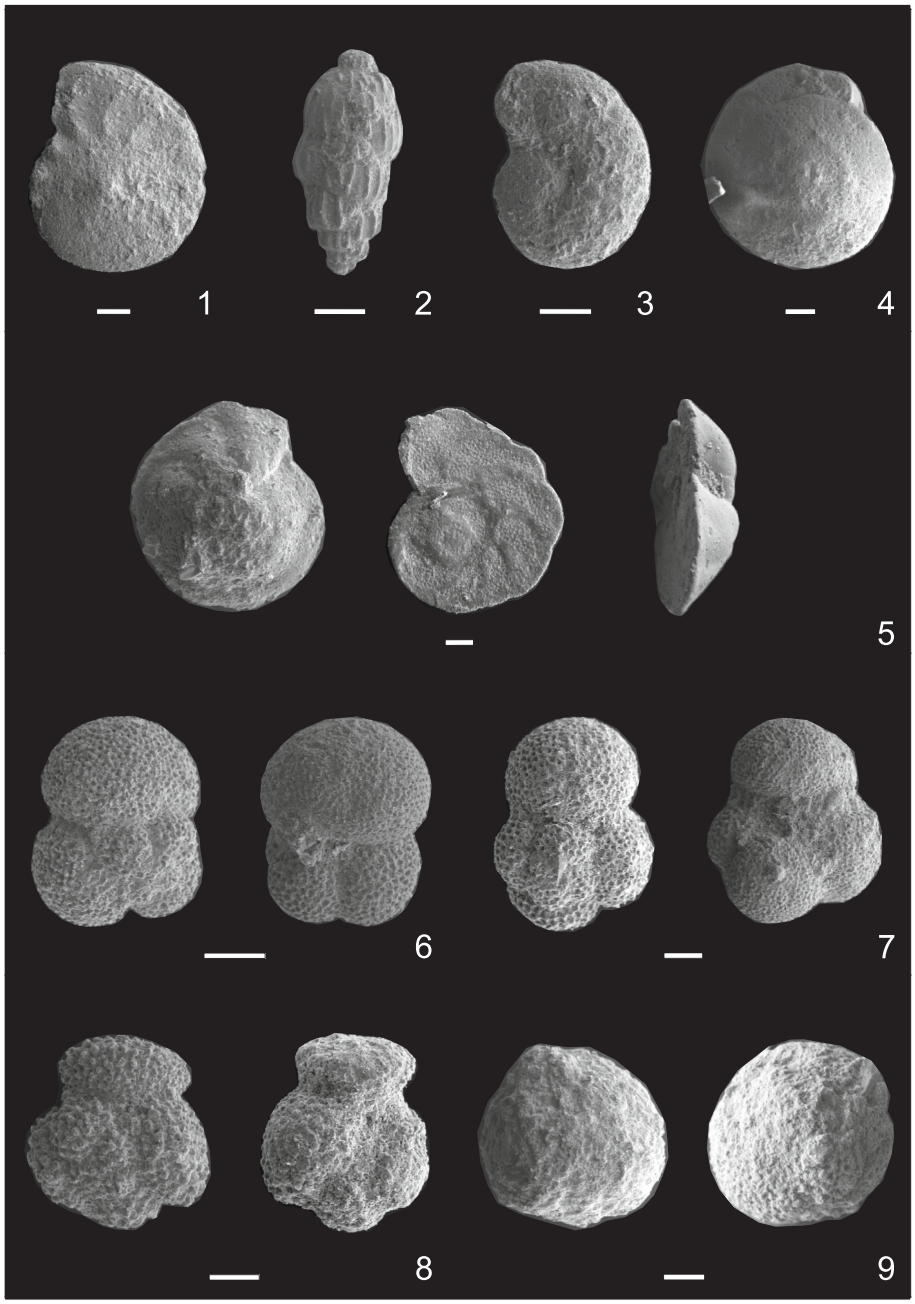

Fig. 7. Scanning electron microscope (SEM) images of the most significant taxa retrieved in this study in the Capo Mortola section. Scale bars of 100 μm apply to all figs. 1) *Operculina* sp.; 2) *Uvigerina* sp.; 3) *Anomalinoides* sp.; 4) *Heterolepa dutemplei* (d'Orbigny, 1846); 5) *Cibicidoides* sp. 6) *Subbotina eocaena* (Guembel, 1868); 7) *Subbotina hagni* (Gohrbandt, 1967); 8) *Acarinina praetopilensis* (Blow, 1979); and 9) *Orbulinoides beckmanni* (Saito, 1962).

2024), but still within the photic zone. At such depths, the genus *Nummulites* is known to be less abundant, and along the section it disappears almost completely as soon as *Discocyclina* becomes abundant. The genus *Operculina* is almost absent in the pre-MECO phase, but it becomes very abundant across the MECO onset. A similar trend is followed by the genus *Discocyclina* (Fig. 1), which becomes quite abundant immediately after the beginning of the MECO onset and occurs in rock-forming amounts, especially from meter 40.0 to 45.0 along the section. Orthophragmines are so abundant that domichnion traces of *Nummipera* are solely constituted by their tests (Fig. 1B3), building amazing structures preserved in situ. Such a sudden increase in the abundance of LBF tests (i.e., both *Operculina* and *Discocyclina*) may point to peculiar environmental conditions related to their specific physiology. The MECO warming might have caused an enhanced hydrological cycle, which could have provided specific advantaged for these foraminifera: continuous flux of nutrients and significant seafloor irradiation reduction. It is so far under debate whether symbionts in discocyclinids could have preferred a light nutrient input as additional intake beside photosynthesis (Molina et al., 2016; Briguglio et al., 2017; Briguglio and Rögl, 2018; Kövecsi et al., 2022; Arena et al., 2024), but this seems evident in some modern oligophotic symbiont-bearing benthic foraminifera (Eder et al., 2017, 2018, 2019; Hohenegger et al., 2019). The continuous flux in nutrient supply and terrigenous influx could easily contribute to the sudden reduction of seafloor irradiation, thus favoring LBF taxa that are usually considered deeper dwellers in the depth gradient, such as orthophragmines, which could move to shallower depths adapting to specific irradiation levels (Egger et al., 2013).

The abundance of *Discocyclina* agamonts is very high, as observed in

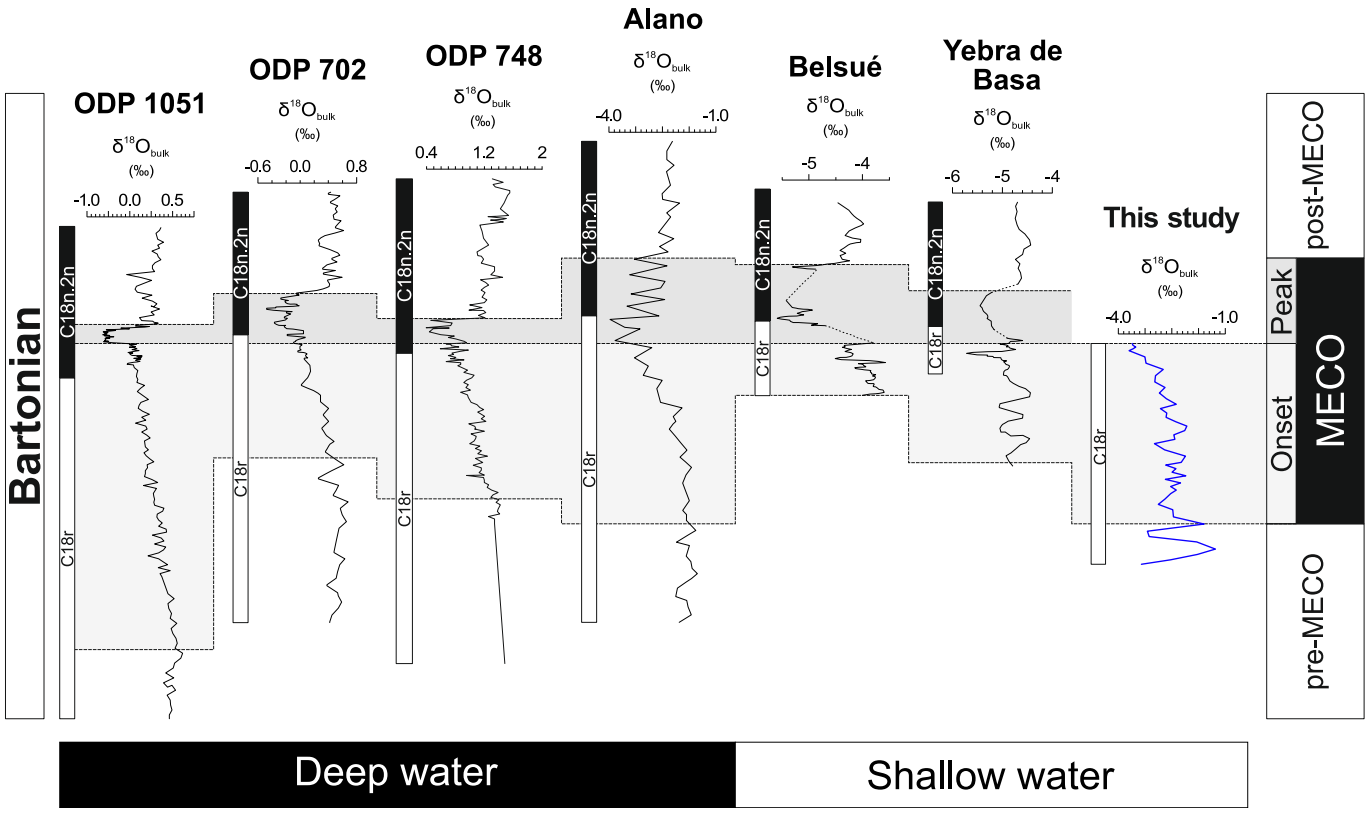

Fig. 8. Stratigraphic correlation of $\delta^{18}O$ between the Capo Mortola section (this study) and global $\delta^{18}O$ records during the MECO, both in deep- and shallow-water environments. Records from correlated sites show the onset and peak of the MECO: Atlantic Ocean: ODP 1051, ODP 702, and ODP 748 (Bohaty et al., 2009); Italy: Alano (Spofforth et al., 2010); Spain: Belsué and Yebra de Basa (Peris-Cabré et al., 2023). The light, gray-shaded band marks the onset of the MECO, whereas the dark gray-shaded band shows the peak of the MECO.

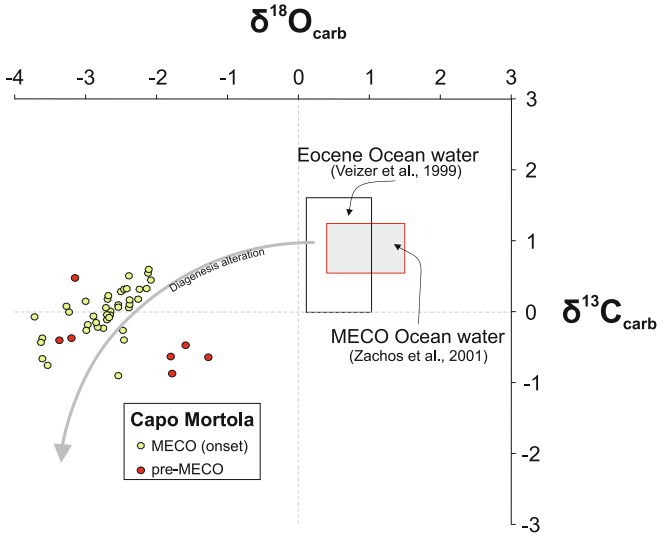

Fig. 9. Cross-plot of carbonate $\delta^{13}C$ vs. $\delta^{18}O$ isotope ratios for the middle Eocene of the Capo Mortola section, showing the pre-MECO interval and the onset of the MECO event. Seawater $\delta^{13}C$ and $\delta^{18}O$ ranges as reported by Veizer et al. (1999) and Zachos et al. (2001) for the Eocene and the MECO. The gray arrow displays the alteration pathway in seawater.

the field (see Fig. B2) and suggests low hydrodynamic conditions on the seafloor (Seddighi et al., 2015; Briguglio et al., 2017); in fact, agamonts are favored in low hydrodynamic settings as gametes have higher chances of merging after the gamonts' reproduction (Briguglio et al., 2017).

Our data suggest that the sudden increase of *Operculina* and *Discocyclina* and the demise of *Nummulites* were not solely controlled by a deepening of the depositional setting; in fact, P/B values and the benthic foraminiferal assemblages do not support significant changes in paleodepth (Fig. 6). Furthermore, if depth was the controlling factor, the ecological replacement in LBF would have been much smoother and not as abrupt as is visible in the succession.

5.3. Environmental conditions in the upper water column

At the Capo Mortola succession, planktic foraminifera are not abundant (see also the P/B ratio in Fig. 6); this is somehow expected in a shallow-water succession dominated by LBF.

The genus *Subbotina* is the most abundant taxon among planktic foraminiferaand is regarded as a deep-water thermocline dweller (e.g., Pearson et al., 2006; D'Onofrio et al., 2021) (Fig. 6). We cannot exclude the possibility that subbotinids may have moved higher in the upper column, as suggested by the stable isotope data from Northwest Atlantic Site U1408 (Kearns et al., 2021). Nonetheless, *Subbotina* is not only recognized as a cold-water index but may also indicate meso- to eutrophic conditions (e.g., Pearson et al., 2006; D'Onofrio et al., 2021). Within the MECO onset, the lower abundance of *Subbotina* could be related to the rise in temperature. However, *Subbotina* keeps slowly up (Fig. 6), and it is reasonable to suppose that it was initially affected by the incipient warming, but afterwards it probably benefited from the nutrient supply related to the enhanced hydrological cycle, commonly associated with warming events (D'Onofrio et al., 2021). The abundance of this genus in pre-MECO is possibly related to a relatively eutrophic environment, as also suggested by the moderately low abundance of LBF or to the colder pre-MECO conditions.

The decline in abundance of *Acarinina* across the MECO onset here

recorded appears unusual for a warm-water index genus (e.g., Pearson et al., 2001, 2006) that could have benefited from the warming trend and needs different explanations. A reduction of the symbiotic relationship (bleaching) of *Acarinina* was documented during the peak of the MECO for ~100 kys at Sites 748 and 1051 (Southern Ocean and mid-latitude North Atlantic, respectively) by Edgar et al. (2013). These authors relate this bleaching episode to the ecological stress induced by increased sea-surface temperatures. However, the Capo Mortola section does not record the MECO peak of temperature; therefore, it seems unlikely that a bleaching episode caused the decrease in abundance of *Acarinina*. Nevertheless, a marked decline of *Acarinina* was also observed in other deep-sea sediments, e.g., in the middle-bathyal Baskil (eastern Turkey) and Alano sections (north-eastern Italy) (Luciani et al., 2010; D'Onofrio et al., 2021). It has been suggested that modifications in salinity and a rise in eutrophic conditions, associated with freshwater input due to the intensified hydrological cycle, impacted the habitat of the specialized, oligotrophic mixed-layer dweller acarininids (e.g., Boersma et al., 1987; Pearson et al., 1993, 2001, 2006; D'Onofrio et al., 2021). It is reasonable to suppose that all these factors recorded in those sections may be the reason behind the decline of *Acarinina* in Capo Mortola and possibly for the rise of *Subbotina*.

The sporadic occurrence of *Morozovelloides* and *O. beckmanni* within the MECO onset does not permit further interpretations. Nevertheless, they are recognized as warm-water indicators that dominated the tropical and subtropical assemblages in the upper Paleocene to middle Eocene (Boersma et al., 1987; Pearson et al., 1993, 2001; Edgar et al., 2010).

In this study, as in the Sealza section (Gandolfi et al., 2023), the absence of *Globigerinatheka* is another atypical feature, especially considering that several species of this genus should co-occur with *O. beckmanni*, which is considered the end member of the *Globigerinatheka curryi-euganea* lineage (Proto Decima and Bolli, 1970). This genus is regarded as a symbiont-bearing mixed layer dweller, recording depleted $\delta^{18}O$ and enriched $\delta^{13}C$ values (Boersma et al., 1987; Pearson et al., 1993; Premoli Silva and Jenkins, 1993; Pearson et al., 2001; Wade and Kroon, 2002; Wade, 2004), thus possibly comparable for its ecological requirements and significance with *Acarinina*. However, the genus *Acarinina* is recorded, though in low abundance, throughout the Capo Mortola section, whereas *Globigerinatheka* is completely absent. The hypothesis that the increased nutrient supply at the MECO onset may have prevented *Globigerinatheka* from thriving does not explain the absence of this genus below the MECO interval. The reasons for its absence are probably related to a different ecological behavior of *Globigerinatheka* with respect to *Orbulinoides beckmanni*, as supposed for the Sealza section (Gandolfi et al., 2023). Following the supposition that *Subbotina* migrated upward in the water column to occupy a similar habitat as *Globigerinatheka* (Kearns et al., 2021), it is not excluded that the latter lost the competition with *Subbotina*. The supposed eutrophication at Capo Mortola was much less intense with respect to the MECO interval from the deep-water Alano section, as we do not record the occurrence of highly opportunistic and eutrophic taxa such as *Chiloguembelina, Jenkinsina,* and *Pseudoglobigerinella bolivariana*, conversely recorded in high abundance at Alano (Luciani et al., 2010; D'Onofrio et al., 2021).

Although the calcareous nannofossil assemblages were only semi-quantitatively estimated and show variable preservation, some changes may give information on variations in the photic zone on the basis of the recognized ecological affinities of the taxa recorded. Specifically, enhanced temperature and eutrophy at the MECO onset can be deduced by the increase in abundance of *Dictyococcites scrippsae* and by the occurrence of *D. bisectus* (that was not detected in the interval below), as these taxa have been considered adapted to warm and eutrophic waters (Wei and Wise, 1990; Villa et al., 2008) (see Supplementary data). In this interval, this assumption is supported by the virtual absence of oligotrophic taxa such as *Sphenolithus furcatulithoides*, *Cyclicargolithus floridanus*, and *Zygrhablithus bijugatus* (Young, 1998; Aubry, 1998; Bralower, 2002; Agnini et al., 2007; Gibbs et al., 2004). In addition, reworking of Cretaceous nannofossils increases at the base of the MECO onset, which is a further signal of transient enrichment in nutrients (see Supplementary data). Similar variations have been detected in the MECO of the Baskil section in Turkey (D'Onofrio et al., 2021).

6. Conclusions

This work provides a significant opportunity to examine the MECO in the shallow-water context of the Capo Mortola section (NW Italy) and assess the resilience of the examined groups to this environmental perturbation. The recorded response allows an interesting comparison with the record from the most widely analyzed deep-water settings.

The MECO interval was identified by means of the calcareous plankton biostratigraphy and the oxygen stable isotope signal, which displays a marked negative excursion of ~1‰ in the interval from 39.20 to 49.30 m. This negative excursion is included within biozone E12 as well as within biozones CNE14 and 15, which largely correspond to the MECO event. However, the correlation of our $\delta^{18}O$ curve with those from deep-sea settings indicates that our succession corresponds only to the onset of the MECO.

Our records on smaller benthic foraminifera from Capo Mortola highlight that they were not particularly sensitive to the initial MECO perturbance because only minor variations in nutrient supply and no de-oxygenation at the seafloor were detected. In turn, the LBF fauna shifted to a new ecological regime during the MECO perturbation and demonstrated resilience. Indeed, the genera *Operculina* and *Discocyclina* became very abundant across the MECO onset; this suggests that the increase in temperature, coupled with additional nutrient supply, created a suitable environment where oligophotic LBF could thrive. The accumulation of abundant agamonts indicates low hydrodynamic conditions with the absence of bottom currents that would have prevented sexual reproduction by fusion of gametes. The supposed enhanced eutrophy, though moderate, to explain the calcareous plankton foraminiferal record does not contrast with the general oligotrophic conditions recorded by smaller benthic foraminifera and whether nutrients were mainly consumed by the former groups.

Interestingly, the variation in planktic foraminiferal abundance recorded at Capo Mortola shows some similarities with those analyzed from other areas of the Tethys that record an increase of subbotinids and a decrease of acarininids as well (Luciani et al., 2010; D'Onofrio et al., 2021). These changes have been tentatively related, in agreement with our scenario, mainly to an increased nutrient supply that, however, was much less intense in the Capo Mortola setting, possibly due to the distance from the fluvial input associated with a different paleogeography.

Our analysis emphasizes that the biotic response to the MECO perturbance is complex and reflects both the dissimilar adaptability of the diverse taxa and the different regional settings.

CRediT authorship contribution statement

Antonella Gandolfi: Writing – review & editing, Writing – original draft, Visualization, Methodology, Investigation, Formal analysis, Data curation, Conceptualization. **Victor Manuel Giraldo-Gómez:** Writing – review & editing, Writing – original draft, Investigation, Conceptualization. **Valeria Luciani:** Writing – review & editing, Conceptualization. **Michele Piazza:** Writing – review & editing. **Valentina Brombin:** Formal analysis. **Simone Crobu:** Investigation, Data curation. **Cesare Andrea Papazzoni:** Writing – review & editing. **Johannes Pignatti:** Writing – review & editing, Validation. **Antonino Briguglio:** Writing – review & editing, Validation, Supervision, Resources, Funding acquisition, Conceptualization.

Declaration of competing interest

The authors declare that they have no known competing financial interests or personal relationships that could have appeared to influence the work reported in this paper.

Data availability

Data will be made available on request.

Acknowledgments

This study was supported by the University of Genova, which funded a Curiosity Driven Project awarded to AB on Ligurian Palaeoenvironments and by the Ministry of Education, University and Research (MIUR), Italy, which awarded to AB, MP, VL and CAP a research project PRIN 2017 labelled "Biota resilience to global change: biomineralization of planktic and benthic calcifiers in the past, present and future" (prot.2017RX9XXY) and a PhD PON Green awarded to AG. VL was supported by FAR 2023 and MP thanks FRA 2022 at the University of Genova for the support of this project. We thank the Hanbury Botanical Gardens Regional Protected Area for sampling permission (52863) and for all the logistical help during the last 4 years of site visits. We would also like to thank Wolfgang Eder (formerly at the University of Genova), Sulia Goeting (University of Lausanne), and Eleni Lutaj (University of Genova) for their help in the fieldwork. The suggestions of both Editor and anonymous Reviewers increased the quality of the earlier draft and they are acknowledged.

Appendix A. Supplementary data

Stratigraphy and distribution of foraminifera and calcareous nannofossils along the Capo Mortola section. Supplementary data to this article can be found online at https://doi.org/10.1016/j.marmicro.2024.102388.

References

Agnini, C., Fornaciari, E., Rio, D., Tateo, F., Backman, J., Giusberti, L., 2007. Responses of calcareous nannofossil assemblages, mineralogy and geochemistry to the environmental perturbations across the Paleocene/Eocene boundary in the venetian Pre-Alps. Mar. Micropaleontol. 63, 19–38.

Agnini, C., Fornaciari, E., Raffi, I., Catanzariti, R., Pälike, H., Backman, J., Rio, D., 2014. Biozonation and biochronology of Paleogene calcareous nannofossils from low and middle latitudes. Newsl. Stratigr. 47 (2), 131–181. https://doi.org/10.1127/0078-0421/2014/0042.

Agnini, C., Backman, J., Boscolo-Galazzo, F., Condon, D.J., Fornaciari, E., Galeotti, S., Giusberti, L., Grandesso, P., Lanci, L., Luciani, V., Monechi, S., Muttoni, G., Pälike, H., Pampaloni, M.L., Papazzoni, C.A., Pearson, P.N., Pignatti, J., Premoli Silva, I., Raffi, I., Rio, D., Rook, L., Sahy, D., Spofforth, D.J.A., Stefani, C., Wade, B.S., 2021. Proposal for the Global Boundary Stratotype Section and Point (GSSP) for the Priabonian Stage (Eocene) at the Alano section (Italy). Episodes 44 (2), 151–173. https://doi.org/10.18814/epiiugs/2020/020074.

Anagnostou, E., John, E.H., Edgar, K.M., Foster, G.L., Ridgwell, A., Inglis, G.N., Pancost, R.D., Lunt, D.J., Pearson, P.N., 2016. Changing atmospheric CO_2 concentration was the primary driver of early Cenozoic climate. Nature 533 (7603), 380–384. https://doi.org/10.1038/nature17423.

Arena, L., Giraldo-Gómez, V.M., Baucon, A., Piazza, M., Papazzoni, C.A., Pignatti, J., Gandolfi, A., Briguglio, A., 2024. Short-term middle Eocene (Bartonian) paleoenvironmental changes in the sedimentary succession of Olivetta San Michele (NW Italy): the response of shallow-water biota to climate in NW Tethys. Facies 70 (4), 259–284. https://doi.org/10.1007/s10347-023-00677-4.

Aubry, M.P., 1998. Early Paleogene calcareous nannoplankton evolution: a tale of climatic amelioration. In: Aubry, M.P., Lucas, S.G., Berggren, W.A. (Eds.), Late Paleocene-Early Eocene Biotic and Climatic Events in the Marine and Terrestrial Records. Columbia University Press, New York, NY, USA, pp. 158–201.

Barr, I.D., Spagnolo, M., Rea, B.R., Bingham, R.G., Oien, R.P., Adamson, K., Ely, J.C., Mullan, D.J., Pellitero, R., Tomkins, M.D., 2022. 60 million years of glaciation in the Transantarctic Mountains. Nat. Commun. 13 (1), 5526.

Bijl, P.K., Houben, A.J., Schouten, S., Bohaty, S.M., Sluijs, A., Reichart, G.J., Sinninghe Damsté, J.S., Brinkhuis, H., 2010. Transient Middle Eocene atmospheric CO_2 and temperature variations. Science 330, 819–821. https://doi.org/10.1126/science.1193654.

Boersma, A., Premoli Silva, I., Shackleton, N.J., 1987. Atlantic Eocene planktonic foraminiferal paleohydrographic indicators and stable isotope paleoceanography. Paleoceanography 2, 287–331. https://doi.org/10.1029/PA002i003p00287.

Bohaty, S.M., Zachos, J.C., 2003. Significant Southern Ocean warming event in the late middle Eocene. Geology 31, 1017–1020. https://doi.org/10.1130/G19800.1.

Bohaty, S.M., Zachos, J.C., Florindo, F., Delaney, M.L., 2009. Coupled greenhouse warming and deep-sea acidification in the middle Eocene. Paleoceanography 24, PA2207. https://doi.org/10.1029/2008PA001676.

Borelli, C., Cramer, B.S., Katz, M.E., 2014. Bipolar Atlantic deep-water circulation in the middle late Eocene: Effects of Southern Ocean gateway openings. Paleoceanography 29, 308–327. https://doi.org/10.1002/2012PA002444.

Boscolo Galazzo, F., Giusberti, L., Luciani, V., Thomas, E., 2013. Paleoenvironmental changes during the Middle Eocene Climatic Optimum (MECO) and its aftermath: the benthic foraminiferal record from the Alano section (NE Italy). Palaeogeogr. Palaeoclimatol. Palaeoecol. 378, 22–35. https://doi.org/10.1016/j.palaeo.2013.03.018.

Boscolo Galazzo, F., Thomas, E., Pagani, M., Warren, C., Giusberti, L., 2014. The middle Eocene climatic optimum (MECO): a multi-proxy record of paleoceanographic changes in the southeast Atlantic (ODP Site 1263, Walvis Ridge). Paleoceanography 29, 1143–1161.

Boussac, J., 1912. Études stratigraphiques sur le Nummulitique alpin. In: Mémoires pour servir à l'explication de le Carte géologique détaillée de la France, 662 pp.

Bown, P.R., Young, J.R., 1998. Techniques. In: Bown, P.R. (Ed.), Calcareous Nannofossil Biostratigraphy. Kluwer Academic, London, pp. 16–28.

Brachert, T.C., Agnini, C., Gagnaison, C., Gély, J.P., Henehan, M.J., Westerhold, T., 2023. Astronomical pacing of middle Eocene sea-level fluctuations: Inferences from shallow-water carbonate ramp deposits. Paleoceanogr. Paleoclimatol. 38, e2023PA004633 https://doi.org/10.1029/2023PA004633.

Bralower, T.J., 2002. Evidence of surface water oligotrophy during the Paleocene-Eocene thermal maximum: Nannofossil assemblage data from Ocean Drilling Program Site 690, Maud Rise, Weddell Sea. Paleoceanography 17, 1023. https://doi.org/10.1029/2001PA000662.

Briguglio, A., Rögl, F., 2018. The Miocene (Burdigalian) Operculinids of Channa Kodi, Padappakkara, Southern India. Palaeontographica (A) 312 (1–4), 17–39.

Briguglio, A., Seddighi, M., Papazzoni, C.A., Hohenegger, J., 2017. Shear versus settling velocity of recent and fossil larger foraminifera: new insights on nummulite banks. Palaios 32, 321–329.

Carbone, F., Giammarino, S., Matteucci, R., Schiavinotto, F., Russo, A., 1981. Ricostruzione paleoambientale dell'affioramento nummulitico di Capo Mortola. Annali dell'Università di Ferrara, (serie 9) 6(suppl.), 231–268.

Coletti, G., Mariani, L., Garzanti, E., Consani, S., Bosio, G., Vezzoli, G., Hu, X., Basso, D., 2021. Skeletal assemblages and terrigenous input in the Eocene carbonate systems of the Nummulitic Limestone (NW Europe). Sediment. Geol. 425, 106005 https://doi.org/10.1016/j.sedgeo.2021.106005.

Coxall, H.K., Wilson, P.A., Pälike, H., Lear, C.H., Backman, J., 2005. Rapid stepwise onset of Antarctic glaciation and deeper calcite compensation in the Pacific Ocean. Nature 433, 53–57. https://doi.org/10.1038/nature03135.

Cramer, B.S., Toggweiler, J.R., Wright, J.D., Katz, M.E., Miller, K.G., 2009. Ocean overturning since the Late Cretaceous: inferences from a new benthic foraminiferal isotope compilation. Paleoceanography 24 (4), PA4216. https://doi.org/10.1029/2008PA001683.

Dallagiovanna, G., Fanucci, F., Pellegrini, L., Seno, S., Bonini, L., Decarlis, A., Maino, M., Morelli, D., Toscani, G., con contributi di Breda, A, Vercesi, P.L., Zizioli, D., Cobianchi, M., Mancin, N., Papazzoni, C.A., 2012a. Note illustrative della Carta Geologica d'Italia alla scala 1:50000, Foglio 257 e 270 Dolceacqua – Ventimiglia. Regione Liguria e ISPRA, 103 pp. https://www.isprambiente.gov.it/Media/carg/note_illustrative/257_270_Dolceacqua_Ventimiglia.pdf.

de Graciansky, P.C., Roberts, D.G., Tricart, P., 2010. The Western Alps, from Rift to Passive Margin to Orogenic Belt: An Integrated Geoscience Overview. Developments in Earth Surface Processes 14. Elsevier, Amsterdam, 398 pp.

D'Onofrio, R., Zaky, A.S., Frontalini, F., Luciani, V., Catanzariti, R., Francescangeli, F., Jovane, L., 2021. Impact of the Middle Eocene Climatic Optimum (MECO) on foraminiferal and calcareous nannofossil assemblages in the Neo-Tethyan Baskil Section (Eastern Turkey): paleoenvironmental and paleoclimatic reconstructions. Appl. Sci. 11 (23), 11339.

Eder, W., Hohenegger, J., Briguglio, A., 2017. Depth-related morphoclines of megalospheric test of *Heterostegina depressa* d'Orbigny: biostratigraphic and palaeobiological implications. Palaios 32, 110–117.

Eder, W., Hohenegger, J., Briguglio, A., 2018. Test flattening in the larger foraminifer *Heterostegina depressa*: predicting bathymetry from axial sections. Paleobiology 44, 76–88.

Eder, W., Woeger, J., Kinoshita, S., Hohenegger, J., Briguglio, A., 2019. Growth estimation of the larger foraminifer *Heterostegina depressa* by means of population dynamics. PeerJ 6, e6096.

Edgar, K.M., Wilson, P.A., Sexton, P.F., Suganuma, Y., 2007. No extreme bipolar glaciation during the main Eocene calcite compensation shift. Nature 448, 908–911.

Edgar, K.M., Wilson, P.A., Sexton, P.F., Gibbs, S.J., Roberts, A.P., Norris, R.D., 2010. New biostratigraphic, magnetostratigraphic and isotopic insights into the Middle Eocene Climatic Optimum in low latitudes. Palaeogeogr. Palaeoclimatol. Palaeoecol. 297, 670–682. https://doi.org/10.1016/j.palaeo.2010.09.016.

Edgar, K.M., Bohaty, S.M., Gibbs, S.J., Sexton, P.F., Norris, R.D., Wilson, P.A., 2013. Symbiont 'bleaching' in planktic foraminifera during the Middle Eocene Climatic Optimum. Geology 41 (1), 15–18.

Egger, H., Briguglio, A., Rögl, F., Darga, R., 2013. The basal Lutetian transgression on the Tethyan shelf of the European craton (Adelholzen beds, Eastern Alps, Germany). Newslett. Stratigr. 46 (3), 287–301.

Fio, K., Spangenberg, J.E., Vlahović, I., Sremac, J., Velić, I., Mrinjek, E., 2010. Stable isotope and trace element stratigraphy across the Permian–Triassic transition: a redefinition of the boundary in the Velebit Mountain, Croatia. Chem. Geol. 278, 38–57.

Fornaciari, E., Agnini, C., Catanzariti, R., Rio, D., Bolla, E.M., Valvasoni, E., 2010. Mid latitude calcareous nannofossil biostratigraphy and biochronology across the middle to late Eocene transition. Stratigraphy 7, 229–264.

Gandolfi, A., Giraldo-Gómez, V.M., Luciani, V., Piazza, M., Adatte, T., Arena, L., Brahimsamba, B., Fornaciari, E., Frijia, G., Kocsis, L., Briguglio, A., 2023. The Middle Eocene Climatic Optimum (MECO) impact on the benthic and planktic foraminiferal resilience from a shallow-water sedimentary record. Riv. Ital. Paleontol. Stratigr. 129 (3), 629–651. https://doi.org/10.54103/2039-4942/20154.

Gèze, B., Lanteaume, M., Peyre, Y., Vernet, J., Nestéroff, W., 1968. Carte géologique de la France au 1/50.000, Feuille Menton-Nice, XXXVII-42 et 43. B.R.G.M. Orléans, 17 pp.

Giammarino, S., Fanucci, F., Orezzi, S., Rosti, D., Morelli, D., Cobianchi, M., De Stefanis, A., Di Stefano, A., Finocchiaro, F., Fravega, P., Piazza, M., Vannucci, G., 2010. Note Illustrative della Carta Geologica d'Italia alla scala 1:50.000 - Foglio "San Remo" n.258- 271. ISPRA - Regione Liguria, 130 pp. A.T.I. - SystemCart s.r.l. - L.A.C. s.r.l. - S.EL.CA, Firenze.

Gibbs, S., Shackleton, N., Young, J., 2004. Orbitally forced climate signals in mid-Pliocene nannofossil assemblages. Mar. Micropaleontol. 51, 39–56.

Giorgioni, M., Jovane, L., Rego, E.S., Rodelli, D., Frontalini, F., Coccioni, R., Catanzariti, R., Özcan, E., 2019. Carbon cycle instability and orbital forcing during the Middle Eocene Climatic Optimum. Sci. Rep. 9, 9357. https://doi.org/10.1038/s41598-019-45763-2.

Giraldo-Gómez, V.M., Beik, I., Podlaha, O.G., Mutterlose, J., 2017. The micropaleontological record of marine early Eocene oil shales from Jordan. Palaeogeogr. Palaeoclimatol. Palaeoecol. 485, 723–739. https://doi.org/10.1016/j.palaeo.2017.07.030.

Giraldo-Gómez, V.M., Mutterlose, J., Podlaha, O.G., Speijer, R.P., Stassen, P., 2018a. Benthic foraminifera and geochemistry across the Paleocene-Eocene Thermal Maximum interval in Jordan. J. Foramin. Res. 48 (2), 100–120.

Giraldo-Gómez, V.M., Beik, I., Podlaha, O.G., Mutterlose, J., 2018b. A paleoenvironmental analyses of benthic foraminifera from Upper Cretaceous–lower Paleocene oil shales of Jordan. Cretac. Res. 91, 1–13.

Herb, R., Hekel, H., 1975. Nummuliten aus dem Obereocaen von Possagno. Abhandlungen der Schweizerischen paläontologischen Gesellschaft 97, 113–135.

Hohenegger, J., Kinoshita, S., Briguglio, A., Eder, W., Wöger, J., 2019. Lunar cycles and rainy seasons drive growth and reproduction in nummulitid foraminifera, important producers of carbonate buildups. Sci. Rep. 9 (1), 8286.

Holbourn, A., Henderson, A.S., MacLeod, N., MacLeod, N., 2013. Atlas of Benthic Foraminifera, vol. 654. Wiley-Blackwell, London.

Jovane, L., Florindo, F., Coccioni, R., Dinarès-Turell, J., Marsili, A., Monechi, S., Roberts, A.P., Sprovieri, M., 2007. The middle Eocene climatic optimum event in the Contessa Highway section, Umbrian Apennines, Italy. Geol. Soc. Am. Bull. 119, 413–427.

Katz, M.E., Miller, K.G., Wright, J.D., Wade, B.S., Browning, J.V., Cramer, B.S., Rosenthal, Y., 2008. Stepwise transition from the Eocene greenhouse to the Oligocene icehouse. Nat. Geosci. 1 (5), 329–334.

Kearns, L.E., Bohaty, S.M., Edgar, K.M., Nogué, S., Ezard, T.H.G., 2021. Searching for function: reconstructing adaptive niche changes using geochemical and morphological data in planktonic foraminifera. Front. Ecol. Evol. 9, 679–722. https://doi.org/10.3389/fevo.2021.679722.

Kövecsi, S.A., Less, G., Pleș, G., Bindiu-Haitonic, R., Briguglio, A., Papazzoni, C.A., Silye, L., 2022. Nummulites assemblages, biofabrics and sedimentary structures: the anatomy and depositional model of an extended Eocene (Bartonian) nummulitic accumulation from the Transylvanian Basin (NW Romania). Palaeogeogr. Palaeoclimatol. Palaeoecol. 586, 110751 https://doi.org/10.1016/j.palaeo.2021.110751.

Lanteaume, M., 1968. Contribution à l'étude géologique des Alpes Maritimes franco-italiennes. Mémoires puor servir à l'explication de la Carte géologique détaillée de la France 1–405.

Läuchli, C., Garcés, M., Beamud, E., Valero, L., Honegger, L., Adatte, T., Castelltort, S., 2021. Magnetostratigraphy and stable isotope stratigraphy of the middle-Eocene succession of the Ainsa basin (Spain): new age constraints and implications for sediment delivery to the deep-waters. Mar. Pet. Geol. 132, 105182 https://doi.org/10.1016/j.marpetgeo.2021.105182.

Lavastre, V., Ader, M., Buschaert, S., Petit, E., Javoy, M., 2011. Water circulation control on carbonate-$\delta^{18}O$ records in a low permeability clay formation and surrounding limestones: The Upper Dogger–Oxfordian sequence from the eastern Paris basin, France. Appl. Geochem. 26 (5), 818–827.

Lear, C.H., Bailey, T.R., Pearson, P.N., Coxall, H.K., Rosenthal, Y., 2008. Cooling and ice growth across the Eocene-Oligocene transition. Geology 36 (3), 251–254.

Loeblich, A.R., Tappan, H., 1987. Foraminiferal Genera and their Classification. Van Nostrand Reinhold Company, New York, 2045 pp.

Loeblich, A.R., Tappan, H., 1994. Foraminifera of the Sahul Shelf and Timor Sea. Cushman Foundation for Foraminiferal Research Special Publication 31, 1–661.

Luciani, V., Giusberti, L., Agnini, C., Fornaciari, E., Rio, D., Spofforth, D.J.A., Pälike, H., 2010. Ecological and evolutionary response of Tethyan planktonic foraminifera to the middle Eocene climatic optimum (MECO) from the Alano section (NE Italy). Palaeogeogr. Palaeoclimatol. Palaeoecol. 292, 82–95. https://doi.org/10.1016/j.palaeo.2010.03.029.

Marini, M., Patacci, M., Felletti, F., Decarlis, A., McCaffrey, W., 2022. The erosionally confined to emergent transition in a slope- derived blocky mass-transport deposit interacting with a turbidite substrate, Ventimiglia Flysch Formation (Grès d'Annot System, north-west Italy). Sedimentology 69, 1675–1704.

Marshall, J.D., 1992. Climatic and oceanographic isotopic signals from the carbonate rock record and their preservation. Geol. Mag. 129, 143–160. https://doi.org/10.1017/S0016756800008244.

Miller, K.G., Fairbanks, R.G., Mountain, G.S., 1987. Tertiary oxygen isotope synthesis, sea level history, and continental margin erosion. Paleoceanography 2 (1), 1–19.

Miller, K.G., Kominz, M.A., Browning, J.V., Wright, J.D., Mountain, G.S., Katz, M.E., Sugarman, P.J., Cramer, B.S., Christie-Blick, N., Pekar, S.F., 2005. The Phanerozoic record of global sea-level change. Science 310 (5752), 1293–1298.

Molina, E., Torres-Silva, A.I., Ćorić, S., Briguglio, A., 2016. Integrated biostratigraphy across the Eocene/Oligocene boundary at Noroña, Cuba, and the question of the extinction of orthophragminids. Newslett. Stratigr. 49 (1), 1–14.

Morabito, C., Papazzoni, C.A., Lehrmann, D.J., Payne, J.L., Alramadan, K.A., Morsilli, M., 2024. Carbonate factory response through the MECO (Middle Eocene Climate Optimum) event: Insight from the Apulia Carbonate Platform. Gargano Promontory, Italy. Sediment. Geol. 461, 106575. https://doi.org/10.1016/j.sedgeo.2023.106575.

Morelli, D., Locatelli, M., Corradi, N., Cianfarra, P., Crispini, L., Federico, L., Migeon, S., 2022. Morpho-structural setting of the Ligurian Sea: the role of structural heritage and Neotectonic inversion. J. Mar. Sci. Eng. 10, 1176. https://doi.org/10.3390/jmse10091176.

Murray, J.W., 2006. Ecology and Applications of Benthic Foraminifera. Cambridge University Press, 426 pp.

Özcan, E., Less, G., Báldi-Beke, M., Kollányi, K., Kertész, B., 2006. Biometric analysis of middle and upper Eocene Discocyclinidae and Orbitoclypeidae (Foraminifera) from Turkey and updated orthophragmine zonation in the Western Tethys. Micropaleontology 52 (6), 485–520.

Özcan, E., Yücel, A.O., Erkızan, L.S., Gültekin, M.N., Kayğılı, S., Yurtsever, S., 2022. Atlas of the Tethyan orthophragmines. Mediterran. Geosci. Rev. 4, 3–213.

Papazzoni, C.A., Ćosović, V., Briguglio, A., Drobne, K., 2017. Towards a calibrated larger foraminifera biostratigraphic zonation: celebrating 18 years of the application of shallow benthic zones. Palaios 21, 1–5.

Patterson, P.P., Walter, L.M., 1994. Depletion of ^{13}C in seawater $\sum CO_2$ on modern carbonate platforms: significance for the carbon isotopic record of carbonates. Geology 22, 885–888. https://doi.org/10.1130/0091-7613(1994)022<0885:DOCISC>2.3.CO;2.

Pearson, P.N., Shackleton, N.J., Hall, M.A., 1993. Stable isotope paleoecology of middle Eocene planktonic foraminifera and multispecies isotope stratigraphy, DSDP Site 523, South Atlantic. J. Foraminifer. Res. 23, 123–140.

Pearson, P.N., Ditchfield, P.W., Singano, J., Harcourt-Brown, K.G., Nicholas, C.J., Olsson, R.K., Shackleton, N.J., Hallk, M.A., 2001. Warm tropical sea surface temperatures in the Late Cretaceous and Eocene epochs. Nature 413, 481–488. https://doi.org/10.1038/35097000.

Pearson, P.N., Olsson, R.K., Hemleben, C., Huber, B.T., Berggren, W.A., 2006. Atlas of Eocene Planktonic Foraminifera. In: Cushman Foundation for Foraminiferal Research Special Publication, 41, 513 pp.

Pekar, S.F., Hucks, A., Fuller, M., Li, S., 2005. Glacioeustatic changes in the early and middle Eocene (51–42 Ma): shallow-water stratigraphy from ODP Leg 189 Site 1171 (South Tasman Rise) and deep-sea $\delta^{18}O$ records. Geol. Soc. Am. Bull. 117 (7–8), 1081–1093.

Perch-Nielsen, K., 1985. Cenozoic calcareous nannofossils. In: Bolli, H.M., Saunders, J.B., Perch-Nielsen, K. (Eds.), Plankton Stratigraphy. Cambridge University Press, Cambridge, pp. 427–554.

Peris-Cabré, S., Valero, L., Spangenberg, J.E., Vinyoles, A., Verité, J., Adatte, T., Maxime Tremblin, M., Watkins, S., Sharma, N., Garcés, M., Puigdefàbregas, C., Castelltort, S., 2023. Fluvio-deltaic record of increased sediment transport during the Middle Eocene Climatic Optimum (MECO), Southern Pyrenees, Spain. Clim. Past 19 (3), 533–554. https://doi.org/10.5194/cp-19-533-2023.

Premoli Silva, I., Jenkins, D.G., 1993. Decision on the Eocene-Oligocene boundary stratotype. Episodes 16 (3), 379–382.

Proto Decima, F., Bolli, M.H., 1970. Evolution and variability of *Orbulinoides beckmanni* (Saito). Eclogae Geol. Helv. 63, 883–905.

Rodelli, D., Jovane, L., Özcan, E., Giorgioni, M., Coccioni, R., Frontalini, F., Rego, E.S., Brogi, A., Catanzariti, R., Less, G., Rostami, M.A., 2018. High-resolution integrated magnetobiostratigraphy of a new middle Eocene section from the Neotethys (Elazığ Basin, eastern Turkey). Geol. Soc. Am. Bull. 130 (1–2), 193–207.

Rögl, F., Spezzaferri, S., 2002. Foraminiferal paleoecology and biostratigraphy of the Mühlbach section (Gaindorf Formation, lower Badenian), Lower Austria. Annalen des Naturhistorischen Museums in Wien, (Serie A) 104, 23–75.

Russo, B., Ferraro, L., Correggia, C., Alberico, I., Foresi, L.M., Vallefuoco, M., Lirer, F., 2022. Deep-water paleoenvironmental changes based on early-middle Miocene benthic foraminifera from Malta Island (Central Mediterranean). Palaeogeogr. Palaeoclimatol. Palaeoecol. 586, 110722.

Saltzman, M.R., Thomas, E., 2012. Carbon isotope stratigraphy. In: Gradstein, F., Ogg, J., Schmitz, M.D., Ogg, G. (Eds.), The Geologic Time Scale. Elsevier, Oxford, UK, pp. 207–232. https://doi.org/10.1016/B978-0-444-59425-9.00011-1.

Savian, J.F., Jovane, L., Trindade, R.I.F., Frontalini, F., Coccioni, R., Bohaty, S.M., Wilson, P.A., Florindo, F., Roberts, A., 2013. Middle Eocene Climatic Optimum (MECO) in the Monte Cagnero Section, Central Italy. Latinmag Lett. 3 (Special Issue), 1–8.

Schaub, H., 1981. Nummulites et Assilines de la Téthys paléogène. Taxinomie, phylogenèse et biostratigraphie. Mémoires suisses de Paléontologie 104-106, 1–236.

Schrag, D.P., DePaolo, D.J., Richter, F.M., 1995. Reconstructing past sea surface temperatures: Correcting for diagenesis of bulk marine carbonate. Geochim. Cosmochim. Acta 59, 2265–2278. https://doi.org/10.1016/0016-7037(95)00105-9.

Seddighi, M., Briguglio, A., Hohenegger, J., Papazzoni, C.A., 2015. New results on the hydrodynamic behaviour of fossil *Nummulites* tests from two nummulite banks from

the Bartonian and Priabonian of northern Italy. Bollettino della Società Paleontologica Italiana 54 (2), 103–116.
Seno, S., Fanucci, F., Dallagiovanna, G., Maino, M., Pellegrini, L., Vercesi, P.L., Morelli, D., Savini, A., Migeon, S., Cobianchi, M., Mancin, N., Marini, M., Felletti, F., Decarlis, A., Maino, M., Toscani, G., Breda, A., Zizioli, D., 2012. Carta Geologica d'Italia alla scala 1:50000, Foglio 257 Dolceacqua e Foglio 270 Ventimiglia. Regione Liguria e ISPRA. https://www.isprambiente.gov.it/Media/carg/257_270_DOLCEACQUA_VENTIMIGLIA/Foglio.html.
Serra-Kiel, J., 1984. Estudi dels *Nummulites* del grup de *N. perforatus* (Montfort) (Conques aquitana, catalana i balear). Treballs de la Institució Catalana d'Història Natural 11, 1–244.
Serra-Kiel, J., Hottinger, L., Caus, E., Drobne, K., Ferrández, C., Jauhri, A.K., Less, G., Pavlovec, R., Pignatti, J.S., Samsó, J.M., Schaub, H., Sirel, E., Strougo, A., Tambareau, Y., Tosquella, J., Zakrevskaya, E., 1998. Larger Foraminiferal Biostratigraphy of the Tethyan Paleocene and Eocene. Bulletin de la Société géologique de France 169, 281–299.
Sexton, P.F., Wilson, P.A., Norris, R.D., 2006. Testing the Cenozoic multisite composite $\delta^{18}O$ and $\delta^{13}C$ curves: New monospecific Eocene records from a single locality, Demerara Rise (Ocean Drilling Program Leg 207). Paleoceanography 21 (2). https://doi.org/10.1029/2005PA001253.
Sinclair, H.D., 1997. Tectonostratigraphic model for underfilled peripheral foreland basins: an Alpine perspective. Geol. Soc. Am. Bull. 109, 324–346.
Sluijs, A., Zeebe, R.E., Bijl, P.K., Bohaty, S.M., 2013. A middle Eocene carbon cycle conundrum. Nat. Geosci. 6 (6), 429–434. https://doi.org/10.1038/NGEO1807.
Speijer, R.P., 1994. Extinction and recovery patterns in benthic foraminiferal paleocommunities across the Cretaceous/Paleogene and Paleocene/Eocene boundaries. Geol. Ultraiect. 124, 1–191.
Speijer, R.P., Schmitz, B., 1998. A benthic foraminiferal record of Paleocene sea level and trophic/redox conditions at Gebel Aweina, Egypt. Palaeogeogr. Palaeoclimatol. Palaeoecol. 137 (1–2), 79–101.
Speijer, R.P., Pälike, H., Hollis, C.J., Hooker, J.J., Ogg, J.G., 2020. The Paleogene period. In: Geological Time Scale 2020. Elsevier, pp. 1087–1140.
Spofforth, D.J.A., Agnini, C., Pälike, H., Rio, D., Fornaciari, E., Giusberti, L., Luciani, V., Lanci, L., Muttoni, G., 2010. Organic carbon burial following the middle Eocene climatic optimum in the central western Tethys. Paleoceanography 25 (3), 3210. https://doi.org/10.1029/2009PA001738.
Sztrákos, K., du Fornel, E., 2003. Stratigraphie, paléoécologie et foraminifères du paléogène des Alpes Maritimes et des Alpes de Haute-Provence (Sud-Est de la France). Rev. Micropaleontol. 46, 229–267.
Tripati, A., Backman, J., Elderfield, H., Ferretti, P., 2005. Eocene bipolar glaciation associated with global carbon cycle changes. Nature 436 (7049), 341–346.
van der Boon, A., Kuiper, K.F., van der Ploeg, R., Cramwinckel, M.J., Honarmand, M., Sluijs, A., Krijgsman, W., 2021. Exploring a link between the Middle Eocene Climatic Optimum and Neotethys continental arc flare-up. Clim. Past 17 (1), 229–239.
van der Zwaan, G.J., 1982. Paleoecology of Late Miocene Mediterranean Foraminifera. PhD Thesis,. Utrecht University, Netherlands, 199 pp.
van der Zwaan, G.J., Jorissen, F.J., de Stigter, H.C., 1990. The depth dependency of planktonic/benthic foraminiferal ratios: constraints and applications. Mar. Geol. 95 (1), 1–16.
Varrone, D., 2004. Le prime fasi di evoluzione del bacino di avanfossa alpino: la successione delfinese cretacico-eocenica, Alpi marittime. PhD Thesis (unpublished),. University of Torino.
Varrone, D., Clari, P., 2003. Stratigraphic and paleoenvironmental evolution of the Microcodium Formation and the Nummulitic Limestone in the French-Italian Maritime Alps. Geobios 36, 775–786.
Veizer, J., Ala, D., Azmy, K., Bruckschen, P., Buhl, D., Bruhn, F., Carden, G.A.F., Diener, A., Ebneth, S., Godderis, Y., Jasper, T., Korte, C., Pawellek, F., Podlaha, O.G., Strauss, H., 1999. $^{87}Sr/^{86}Sr$, $\delta\ ^{3}C$ and $\delta\ ^{18}O$ evolution of Phanerozoic seawater. Chem. Geol. 161 (1), 59–88. https://doi.org/10.1016/S0009-2541(99)00081-9.
Villa, G., Fioroni, C., Pea, L., Bohaty, S.M., Persico, D., 2008. Middle Eocene-late Oligocene climate variability: Calcareous nannofossil response at Kerguelen Plateau, Site 748. Mar. Micropaleontol. 69, 173–192.
Wade, B.S., 2004. Planktonic foraminiferal biostratigraphy and mechanisms in the extinction of *Morozovella* in the late middle Eocene. Mar. Micropaleontol. 51 (1–2), 23–38.
Wade, B.S., Kroon, D., 2002. Middle Eocene regional climate instability: evidence from the western North Atlantic. Geology 30 (11), 1011–1014.
Wade, B., Pearson, P.N., Berggren, W.A., Pälike, H., 2011. Review and revision of Cenozoic tropical planktonic foraminiferal biostratigraphy and calibration to the geomagnetic polarity and astronomical time scale. Earth Sci. Rev. 104, 111–142. https://doi.org/10.1016/j.earscirev.2010.09.003.
Wei, W., Wise Jr., S.W., 1990. Biogeographic gradients of middle Eocene-Oligocene calcareous nannoplankton in the South Atlantic Ocean. Palaeogeogr. Palaeoclimatol. Palaeoecol. 79, 29–61.
Westerhold, T., Marwan, N., Drury, A.J., Liebrand, D., Agnini, C., Anagnostou, E., Barnet, J.S.K., Bohaty, S.M., De Vleeschouwer, D., Florindo, F., Frederichs, T., Hodell, D.A., Holbourn, A.E., Kroon, D., Lauretano, V., Littler, K., Lourens, L.J., Lyle, M., Pälike, H., Röhl, U., Tian, J., Wilkens, R.H., Wilson, P.A., Zachos, J.C., 2020. An astronomically dated record of Earth's climate and its predictability over the last 66 million years. Science 369, 1383–1387.
Witkowski, J., Bohaty, S.M., Edgar, K.M., Harwood, D.M., 2014. Rapid fluctuations in mid-latitude siliceous plankton production during the Middle Eocene Climatic Optimum (ODP Site 1051, western North Atlantic). Mar. Micropaleontol. 106, 110–129.
Young, J.R., 1998. Neogene nannofossils. In: Calcareous Nannofossil Biostratigraphy. British Micropalaeontology Society Publications Series. Kluwer Academic Publisher, Cambridge, pp. 225–265.
Young, J.R., Bown, P.R., Lees, J.A., 2022. Nannotax3 Website. International Nannoplankton Association. Accessed 21 Apr. 2022. URL. www.mikrotax.org/Nannotax3.
Zachos, J.C., Quinn, T.M., Salamy, K.A., 1996. High-resolution (10^4 years) deep-sea foraminiferal stable isotope records of the Eocene-Oligocene climate transition. Paleoceanography 11 (3), 251–266.
Zachos, J.C., Pagani, M., Sloan, L.C., Thomas, E., Billups, K., 2001. Trends, rhythms, and aberrations in global climate 65 Ma to present. Science 292, 686–693.
Zachos, J.C., Dickens, G.R., Zeebe, R.E., 2008. An early Cenozoic perspective on greenhouse warming and carbon-cycle dynamics. Nature 451 (7176), 279–283.